*Jpn. J. Genet.* (1995) **70**, *pp.* 233–265

# Theoretical analyses of chiasmata using a novel chiasma graph method applied to Chinese hamsters, mice, and dog

Masayasu Y. WADA[1] and Hirotami T. IMAI[2,*]

[1]*Amagi Wild Boar Park, Amagiyugashima, Shizuoka-ken 410-32*
[2]*National Institute of Genetics, Mishima, Shizuoka-ken 411, Japan*

*(Received 21 November 1994)*

## ABSTRACT

Some basic concepts of chiasma (including chiasma distribution, chiasma frequency, interstitial and terminal chiasmata, and chiasma interference) are reexamined theoretically in the light of gene shuffling, and a new method for chiasma analysis termed the chiasma graph is proposed. Chiasma graphs are developed for three mammals with greatly different chromosome numbers: Chinese hamster (with n=11), mice (n=20), and a dog (n=39). The results demonstrate that interstitial chiasmata can contribute both to gene shuffling and to the binding of bivalents, but that so-called terminal chiasmata are in fact mostly achiasmatic terminal associations, the main function of which is to bind bivalents. For this reason, terminal chiasmata should be excluded when chiasma frequency is estimated. It is also demonstrated that interstitial chiasmata distribute on bivalents randomly and uniformly, except at the centromere and telomere. Interference distance fluctuates almost randomly above a minimum value equivalent to about 1.8% of total bivalent length at diakinesis. These results indicate that chiasma formation in mammals is principally a random event. The demonstrated minimum interference distance seems consistent with the polymerization model for chiasma formation. Some cytological aspects of crossing-over are discussed with reference to the minimum interaction theory for eukaryotic chromosome evolution.

## 1. INTRODUCTION

Genetic recombination, which is familiar to cytogeneticists as crossing-over, is fundamentally important in genetics because it provides a mechanism for gene shuffling. Following the pioneering studies of Morgan (1910) and Sturtevant (1913) crossing-over has played a major role in the mapping of genes on chromosomes. Although modern molecular techniques, such as the fluorescence in situ hybridization (FISH) in combination with chromosome banding, have revolutionized gene mapping, crossing-over remains fundamental in this field of genetics. In this regard there is well established cytological evidence that the crossing-over in eukaryote cells, which initiates at pachytene in the recombination nodules on the synaptonemal complex, is visualized using light microscopy as chiasmata at

---

[*] Corresponding author.

diplotene, diakinesis, and metaphase I (for details see general reviews by Evans and Dickinson, 1984, and Moens, 1987). The close relationship between crossing-over events and chiasmata was first proposed by Janssens (1924) in his chiasma type hypothesis, and later established by Darlington (1932).

Recently, some theoretical models of chiasma interference (King and Mortimer, 1990; Foss et al., 1993; Lande and Stahl, 1993) have been proposed, based on the data relating to crossing-over in *Drosophila melanogaster* (Charles, 1938). Crossing-over in these models is detected indirectly by the appearance of crossover progeny following hybridization. For this reason their methodology cannot directly indicate where or how relevant crossing-over events occurred, excepting intragenic exchange. Moreover, these methods can be applied only to those eukaryotes in which cross-breeding is possible, e.g., *Drosophila*, silkworms, mice, domestic animals, crops, etc. The relevant difficulties would be obviated if there was 1:1 correspondence between genetic recombination, crossing-over and the presence of chiasmata, since chiasmata can be easily resolved in most eukaryotes using light microscopy. The chiasma type hypothesis mentioned above remains, for this reason, attractive to modern cytogeneticists.

Chiasma distribution on bivalents and chiasma frequency per cell are two important cytological parameters for the analysis of crossing-over, and ultimately of genetic recombination. The former provides information on the locations of crossing-over points on chromosomes, and the latter reveals the frequency of gene shuffling.

If chiasmata move to terminals during the first meiotic prophase and metaphase, as assumed by Darlington (1932) in his chiasma terminalization hypothesis, cytological information related to crossing-over would be virtually lost, or at least highly biassed. Many cytologists have supported Darlington's hypothesis, but conclusive evidence denying the occurrence of chiasma terminalization has been obtained using BrdU labeling techniques (Tease and Jones, 1978; Kanda and Kato, 1980: for further details see the review by John, 1990).

It may be argued that recombination nodules (RNs) might provide a more appropriate medium than chiasmata for analysis of the molecular mechanisms of crossing-over. This we do not deny, but we do emphasize that recombination is essentially a stochastic event, where relevant information is measured using statistics such as crossover value or chiasma frequency. Recombination nodules are not always suitable for quantitative statistical analysis of crossing-over, because most appear at early pachytene and are aborted, so that only some are able to contribute to chiasma formation [Fig. 1-(1)] (Holm and Rasmussen, 1980; Rasmussen and Holm, 1984; Stack and Anderson, 1986). This means that chiasmata as cytological phenomena remain potentially valuable for analysis of crossing-over.

Some perplexing problems remain: for example, the nature of pseudochiasma, pseudoterminalization, and terminal chiasma. In a later section we point out that

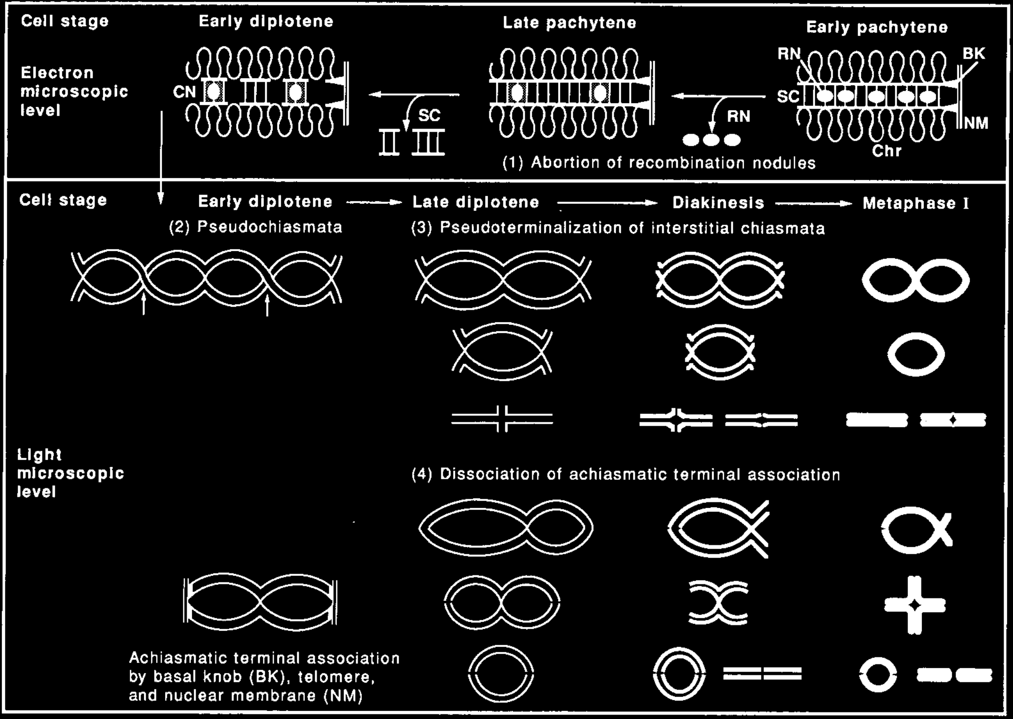
Cell stage
Early diplotene
Late pachytene
Early pachytene
Electron microscopic level
CN
SC
II
III
RN
RN
BK
SC
NM
Chr
(1) Abortion of recombination nodules
Cell stage
Early diplotene
Late diplotene
Diakinesis
Metaphase I
(2) Pseudochiasmata
(3) Pseudoterminalization of interstitial chiasmata
Light microscopic level
(4) Dissociation of achiasmatic terminal association
Achiasmatic terminal association by basal knob (BK), telomere, and nuclear membrane (NM)

Fig. 1. Schematic representation of crossing-over, with initiation at pachytene, chiasma formation at diplotene, and chiasma transformation at diakinesis and metaphase I. Numbered items are factors which bias estimates of crossing-over frequency or the number of chiasmata per cell. BK: basal knob. Chr: (bivalent) chromosome. CN: chromatin nodule. NM: nuclear membrane. RN: recombination nodule. SC: synaptonemal complex.

bivalents are often twisted at early diplotene, and thus it is often difficult to discriminate genuine chiasmata from pseudochiasmata resulting from such torsion [Fig. 1-(2)]. Some bivalents, especially those of small size, and the sex chromosomes, tend to associate end-to-end (see Metaphase I in Fig. 1). This configuration has been conventionally considered as pseudoterminalization of distally localized interstitial chiasmata [Fig. 1-(3); e.g., Jones and Tease, 1984]. In this case, terminal chiasmata are counted in the estimation of chiasma frequency. The alternative hypothesis, that at least some perceived terminal chiasmata are achiasmatic terminal association, was proposed long ago by Janssens (1924), Sax (1930), and Belling (1931). More recently, this concept was reinstated in studies of mice by Imai and Moriwaki (1982), and orthopteran insects with terminal heterochromatin by John and King (1982, 1985). The X-Y associations in marsupials (Sharp, 1982) and some eutherian mammals (Solari and Ashley, 1977; Joseph and Chandley, 1984; Wolf et al., 1988) are known to be indisputably achiasmatic, following electron microscopic analyses. In these cases, the terminal association should not be included when estimating chiasma frequency.

According to Mather (1936, 1937), each bivalent must necessarily be binded by either interstitial or terminal chiasma during the first meiotic prophase and metaphase. In this model, large-sized bivalents are secured mainly by interstitial chiasmata, but small ones are binded preferentially by terminal chiasmata. A simple question arises - do terminal chiasmata contribute to gene shuffling? There is accumulating evidence that chromosome terminals are sealed by tandem arrays of telomeres $(ttaggg)_n$ in higher vertebrates, including mammals. This can be visualized by FISH (Meyne et al., 1990; Moyzis et al., 1988). It is also evident that the centromere has a compound structure, i.e., a 17 base motif of CENP-B box as a binding site to the microtubule is the molecular unit of the centromere (Masumoto et al., 1989a,b), and this unit is repeated many times in alphoid DNA or satellite DNA, which consist of pericentromeric heterochromatin (Kipling et al., 1994). These compound structures of telomeres and centromeres support the idea that DNA exchanges which have occurred in both the centromere and telomere regions of acrocentrics, or the telomere regions of metacentrics do not contribute to gene shuffling. A number of problems involving terminal chiasmata and chiasma frequency thus require further examination.

In this paper we review a new technique for quantitative analysis of chiasmata, named the chiasma graph method, and apply it to the Chinese hamster, the mouse and the dog. We also discuss various problems inherent in conventional chiasma analysis procedures.

## 2. BIOLOGICAL MATERIALS AND CYTOLOGICAL METHODS

For quantitative analysis we use data from three mammalian species with very different chromosome numbers. They are: Chinese hamster (with $2n=22$, $n=11$), a laboratory mouse strain BALB/c (with $2n=40$, $n=20$), and a domestic dog (with $2n=78$, $n=39$). Experimental preparations utilized fresh testes of three mature (6–7 months old) male Chinese hamsters (*Cricetulus griseus*), including a total of 40 cells examined at diplotene, 140 at diakinesis, and 221 at metaphase I. For BALB/c mice, we use data previously published by Imai and Moriwaki (1982). The dog data are considered preliminary, since only 7 cells were examined. We consider, however, that they yielded information sufficient for this project.

Chromosome preparations were made by an improved air-drying technique (Imai et al., 1981). Centromeres were located on bivalents using the modified silver staining method of Howell and Black (1980; for details see Wada and Imai, 1991).

## 3. DEFINITION OF TERMS

### *Size of bivalents*

Let S, L, and Chr respectively be the short arm, long arm, and individual chromosome (bivalent) of a haploid karyotype (Fig. 2a). S, L, and Chr also indicate the dimension of each category, as represented by percentage length versus the total length of autosomal bivalents, where Chr = S + L. The chiasmata of the sex chromosomes were examined here separately from those of autosomes,

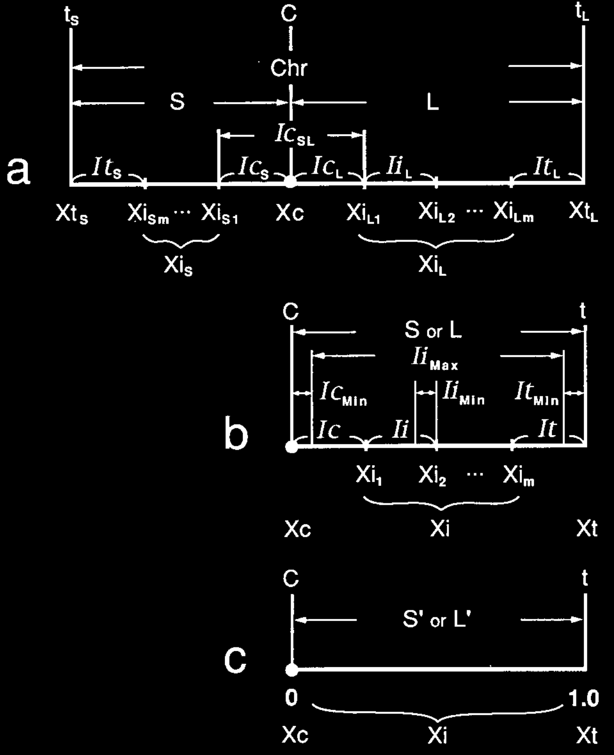

Fig. 2. Terminologies used for chromosome structures and chiasmata in this paper. a, A biarmed chromosome with short (S) and long (L) arm. b, A telocentric chromosome with short or long arms, modified for chiasma distribution graph representation. This was derived from the biarmed chromosome (a) by severance at the centromere. c, A standardized chromosome arm (S' or L' = 1.0). $t_S$: terminus of short arm. $t_L$: terminus of long arm. C: centromere. Chr: individual (bivalent) chromosome, Chr = S + L. X: chiasma. Xt: terminal chiasma. Xi: interstitial chiasma. Xc: centromeric chiasma. $Xi_S$ and $Xi_L$: interstitial chiasmata in short or long arm. $Xi_{Sm}$ and $Xi_{Lm}$: the mth interstitial chiasma from the centromere in a short or a long arm. $I$: (chiasma) interference distance. $It$: terminal interference distance. $Ic$: centromeric interference distance. $Ii$: interstitial interference distance. $Ic_{Min}$ and $It_{Min}$: the minimum centromeric or minimum terminal interference distance. $Ii_{Max}$ and $Ii_{Min}$; the maximum or minimum interstitial interference distance. $Ic_{SL} = Ic_S + Ic_L$. See text and Table 1 for more detailed definitions of terminology.

Table 1. Basic symbols employed

| Symbol | Definition |
|---|---|
| Chromosome morphology and structure | |
| Chr | Individual chromosome and the size of individual chromosome against the total length of autosomal bivalents (Chr=S+L) |
| S | Short chromosome arm and the size of a short arm |
| L | Long chromosome arm and the size of a long arm |
| S' or L' | Standardized short or long arms (S' or L'=1.0) |
| C | Centromere |
| t | Termini of bivalents |
| Classification of chiasma | |
| X | Chiasma or chiasmata |
| Xc | Centromeric chiasma |
| Xi | Interstitial chiasma and the distance of an interstitial chiasma from the centromere |
| $Xi_S$ | Interstitial chiasma(ta) in a short arm |
| $Xi_L$ | Interstitial chiasma(ta) in a long arm |
| Xt | Terminal chiasma |
| $Xt_S$ | Terminal chiasma(ta) in a short arm |
| $Xt_L$ | Terminal chiasma(ta) in a long arm |
| Classification of bivalent | |
| mXi.2Xt bivalent | A bivalent with mXi and 2Xt ($m \geqq 1$) |
| mXi.1Xt bivalent | A bivalent with mXi and 1Xt ($m \geqq 1$) |
| mXi bivalent | A bivalent with mXi ($m \geqq 1$) |
| 2Xt bivalent | A bivalent with two terminal chiasmata ($m=0$) |
| 1Xt bivalent | A bivalent with one terminal chiasma ($m=0$) |
| 0X bivalent | A bivalent with no chiasmata ($m=0$) |
| Classification of chromosome arm (for the chiasma graph) | |
| mXi.1Xt arm | A short or long arm with mXi ($m \geqq 1$) and 1Xt |
| mXi arm | A short or long arm with mXi ($m \geqq 1$) |
| 1Xt arm | A short or long arm with 1Xi ($m=0$) |
| 0X arm | A short or long arm with no chiasmata ($m=0$) |
| Chiasma frequency | |
| FX | Chiasma frequency per cell |
| FXi | Frequency of interstitial chiasmata per cell<br>(=The chiasma frequency per cell proposed in the present paper) |
| FXit | Frequency of interstitial and terminal chiasmata per cell<br>(=The conventional chiasma frequency per cell) |
| FX/b | Chiasma frequency per bivalent |
| FXi/b | Frequency of interstitial chiasmata per bivalent |
| FXit/b | Frequency of interstitial and terminal chiasmata per bivalent |
| Chiasma interference | |
| $I$ | (Chiasma) interference distance |
| $Ic$ | Centromeric interference distance |
| $Ii$ | Interstitial interference distance |
| $It$ | Terminal interference distance |
| $Ic_{\mathrm{Min}}$ | Minimum centromeric interference distance |
| $Ii_{\mathrm{Min}}$ | Minimum interstitial interference distance |
| $It_{\mathrm{Min}}$ | Minimum terminal interference distance |
| $Ii_{\mathrm{Max}}$ | Maximum interstitial interference distance;<br>$Ii_{\mathrm{Max}}=(\mathrm{S}\text{ or }\mathrm{L})-(Ic_{\mathrm{Min}}+It_{\mathrm{Min}})$ |
| Meiotic cell stage | |
| DT | Diplotene |
| DK | Diakinesis |
| MI | Metaphase I |

but they are included in the tally of chiasma frequency per cell. Symbols used below are defined in context and summarized in Table 1.

### *Classification of chiasmata*

Chiasma and chiasmata are conventionally abbreviated as Xa and Xta (e.g., Darlington, 1933; Southern, 1967; John, 1990). We use "X" to both, since distinction is not required. Chiasmata are classified into three categories: centromeric chiasma (Xc), interstitial (Xi), and terminal (Xt).

Xc is basically a theoretical category, since chiasma formation is usually inhibited in the region of the centromere (e.g., Southern, 1967; Hulten, 1974; Jones, 1984; for further details see John, 1990).

Xi is the most important category with regard to gene shuffling.

The term Xt embraces three categories: (1) achiasmatic terminal associations (=TA by Imai and Moriwaki, 1982), (2) end-to-end associations involving pseudoterminalization of interstitial chiasmata (Jones, 1978), and (3) terminal chiasma in its literal sense.

Our classification recognizes some sub-categories, for example: $Xi_S$, $Xi_L$, $Xt_S$, $Xt_L$, $Xi_{S1...Sm}$, and $Xt_{L1...Lm}$, where S and L indicate short and long arms respectively, and the subscript $_{Sm}$ and $_{Lm}$ indicate the mth interstitial chiasma from the centromere in each arm (Fig. 2a). The terms Xc, $Xt_S$, $Xt_L$, $Xi_{S1...Sm}$, and $Xt_{L1...Lm}$ are also used to indicate the location of each chiasma bivalent. Chiasma locations are represented as the distance from the centromere to each chiasma, and are expressed as percent lengths relative to the total length of autosomal bivalents, e.g., $Xc=0$, $Xt_S=S$, $Xt_L=L$, $0<Xi_{Sm}<S$, and $0<Xi_{Lm}<L$. Where there is no need to discriminate short from long arms more simplified terms are applied: for example: Xi, Xt, $Xi_m$, $Xt_m$. The term (S or L) is also used (Fig. 2b).

### *Classification of bivalents by the type of chiasmata*

We classify bivalents into three major types based on the number of relevant Xi and Xt chiasmata involved. They are termed mXi.2Xt, mXi.1Xt, and mXi bivalents, where $m \geqq 0$. We also use 2Xt, 1Xt, and 0X bivalents as special cases at $m=0$. To simplify descriptions, 0Xt and 0Xi are omitted, and 0X is used as the abbreviation of 0Xi.0Xt.

### *Classification of bivalent arms by the type of chiasmata involved*

The chiasma distribution graph method is introduced below. In the graph, short and long arms of meta- and acrocentric bivalents are regarded as two independent "telocentric" bivalents of size S or L, where we use the terms mXi.1Xt, mXi, 1Xt, and 0X arms with analogy to the classification of bivalents presented above.

*Chiasma frequency per cell (FX)*

The term FX is used to introduce chiasma frequency per cell. It is a more general term than FXi and FXit. FXi stands for the total number of interstitial chiasmata (Xi) per cell, and is equivalent to the chiasma frequency term (CF) used by Imai and Moriwaki (1982). FXit stands for conventional chiasma frequency, where both interstitial (Xi) and terminal chiasmata (Xt) are included. In the same way, the chiasma frequency per bivalent is denoted FX/b or FXi/b or FXit/b as required.

*Interference distance (I)*

Following Mather (1936, 1937), we use "*I*" to indicate the distance of chiasma interference (representing a distance between two chiasmata). We recognize three classes of interference distance, namely: interstitial interference distance (*Ii*), terminal interference distance (*It*), and centromeric interference distance (*Ic*) as follows (Fig. 2):

*Ii*: The interference distance between two adjoining interstitial chiasmata. Southern (1967), and Maudlin and Evans (1980) used $i_1$, $i_2$ etc. to distinguish these classes. Since "i" indicates "interstitial" in our nomenclature, we use $Ii_L$, $Ii_S$, $Ii_{L1}$, $Ii_{L2}$, $Ii_{S1}$, $Ii_{S2}$, $Ii_1$, $Ii_2$ etc., where S and L indicate short and long arms, respectively.

*It*: The interference distance between the chromosome terminal and the nearest Xi, or between Xt and the nearest Xi. For more detailed descriptions, we use $It_S$, $It_L$, or $It_{\mathrm{Min}}$. $It_{\mathrm{Min}}$ stands for the minimum terminal interference distance (Fig. 2b), and corresponds to the term *r. t.* (residual telomeric) by Southern (1967), and Maudlin and Evans (1980).

*Ic*: The interference distance between the centromere and the nearest Xi. As mentioned above, *Ic* is mostly resulting from the inhibition of chiasma formation at the centromere. The term *Ic* is synonymous to *r. c.* (residual centric) by Southern (1967), and Maudlin and Evans (1980). We use $Ic_{\mathrm{SL}}$ and $Ic_{\mathrm{Min}}$ as special cases of *Ic*. The former is defined as the interference distance between $\mathrm{Xi_{S1}}$ and $\mathrm{Xi_{L1}}$ (Fig. 2a), and the latter means the minimum centromeric interference distance (Fig. 2b).

## 4. THEORETICAL BASES FOR THE CHIASMA GRAPH

Information relating to chiasma frequency and chiasma distribution is conventionally represented by a histogram recording chiasma frequency per unit arm length (e.g., 5%) in individual bivalents. This method is useful, since it indicates the detailed pattern of chiasma frequency distribution in individuals bivalent. It is difficult, however, to demonstrate any overall tendencies involving chiasma distribution and frequency, even in a single karyotype, let alone in heterogeneous

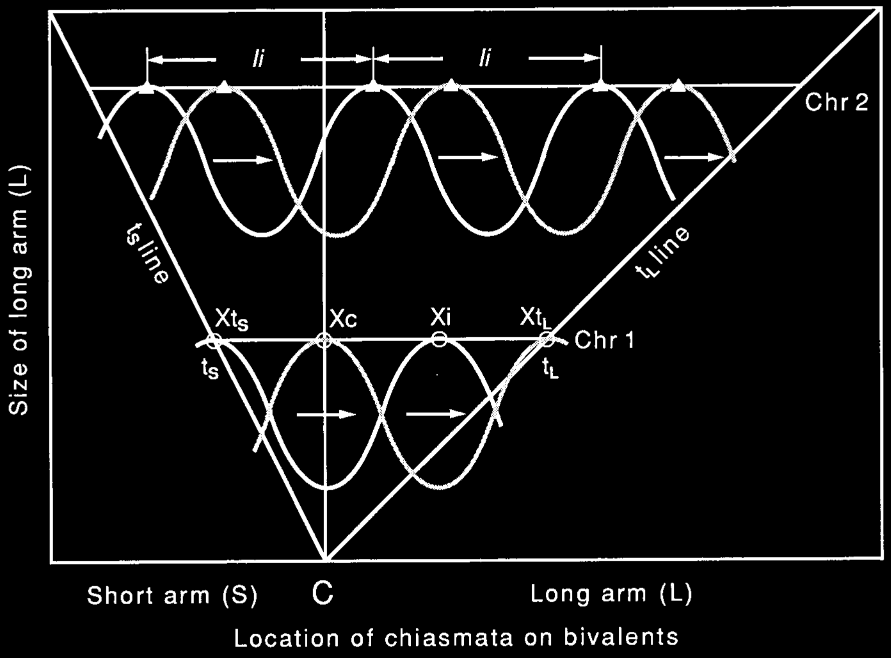

Fig. 3. Preliminary steps in construction of the chiasma distribution graph-(1). Representation of the bivalent chromosomes of a haploid karyotype having only subtelocentrics ($r=1.9$) on a two dimensional graph, and drawing the chiasma location on each bivalent (Chr 1, 2,..), by assuming a constant interstitial interference distance (*Ii*). Interference is indicated by a sine curve, where chiasmata are assumed to occur only at the crests of waves. The potential distribution of chiasmata on each bivalent is estimated by sliding the sine curve to the right (compare solid and meshed curves). $t_S$ and $t_L$ line: trajectories of short or long arm termini. See Fig. 2 for other abbreviations.

karyotypes of different species (e.g., Southern, 1967).

In order to visually demonstrate information concerning chiasma distribution and chiasma frequency, we propose here a new method, termed the "chiasma graph". Two types of chiasma graphs are recognized: the "chiasma distribution graph" and the "chiasma frequency graph". Relevant theoretical details are outlined below.

## A. *Preliminary steps in developing the chiasma distribution graph*

The prototype of the chiasma distribution graph was introduced by Imai and Moriwaki (1982) in an investigation of mice with 20 acrocentric chromosomes. The method is further developed here, in order to represent more general karyotypes including both metacentric (M) and acrocentric (A) chromosomes.

In order to simplify the descriptions, we first consider a chiasma distribution graph based on a hypothetical karyotype possessing only subtelocentric (ST) chromosomes with a constant arm ratio ($r=1.9$) (Fig. 3). The steps for construction of the graph are:

(1) Use bivalents at diakinesis.

(2) Consider a two-dimensional graph in which the ordinate is calibrated to the size of long arms (L) and the abscissa to the size of short (S) or long (L) arms of bivalents (Chr=S+L).

(3) The centromere of each bivalent is plotted at the origin of the abscissa, and the location of chiasmata (Xi or Xt) on the short or long arm is plotted respectively on the right and left sides of the origin. $Xt_S=S$, $Xc=0$, $0<Xi_L<L$, and $Xt_L=L$ following these definitions. For example: in Chr 1 of Fig. 3, Xc, $Xt_S$, and $Xt_L$ are plotted at the points (0, L), (S, L) and (L, L) (see open circles). Chr 1 is represented as a segment of a line with the length (S+L) on the graph, which is parallel to the abscissa.

(4) Bivalents with different sizes distribute in the area between the two border lines given by the trajectories of short and long arm termini (termed the $t_S$ and $t_L$ lines).

If chiasmata occur randomly on each bivalent, and if the given karyotype has bivalents of various sizes, chiasmata will distribute uniformly on the chiasma distribution graph in the area between the $t_S$ and $t_L$ lines (Fig. 3).

### *B. Chiasma distribution in the presence of chiasma interference*

The same uniform distribution of chiasmata is expected even when chiasma interference (*I*) is present. Chiasma interference is shown schematically in Fig. 3 by a sine curve, where chiasmata are assumed to occur only at the peaks of the wave (see open circles or solid triangles). The interstitial interference distance (*Ii*) is equivalent to the distance between two adjacent wave crests. The numbers and locations of interstitial chiasmata in each bivalent are determined by the location of the initial chiasma and *Ii*, e.g., three in Chr 2 (see the solid triangles in Fig. 3). Of course, it is difficult to identify which of the three chiasmata in this example should be regarded as the first, but the same distribution is obtained regardless of this selection. If the first chiasma appears at an arbitrary point on the bivalent, interstitial chiasmata will distribute, in a statistical sense, uniformly on the bivalent. This conclusion can be visually demonstrated on the chiasma graph by moving the sine wave horizontally, parallel to the bivalent (see solid and meshed curves in Fig. 3).

There is a simple relationship between the size of bivalents (Chr), the interstitial interference distance (*Ii*), and the chiasma frequency per bivalent (FXi/b), and this is formulated as $(m\text{-}1)Ii \leqq Chr < mIi \rightarrow FXi/b=(m\text{-}1)$ or m, where $m \geqq 1$. Examples are: $0Ii \leqq Chr < 1Ii \rightarrow FXi/b=0$ or 1, and $1Ii \leqq Chr < 2Ii \rightarrow FXi/b=1$ or 2. For further details see Fig. 4, in which the distributions of chiasma(ta) in 1Xi, 2Xi, 3Xi, and 4Xi bivalents are represented respectively by solid circles, open circles, solid triangles, and open squares. In Fig. 4, the potential distribution areas of chiasmata in mXi bivalents are determined by the parameters Chr and *Ii*,

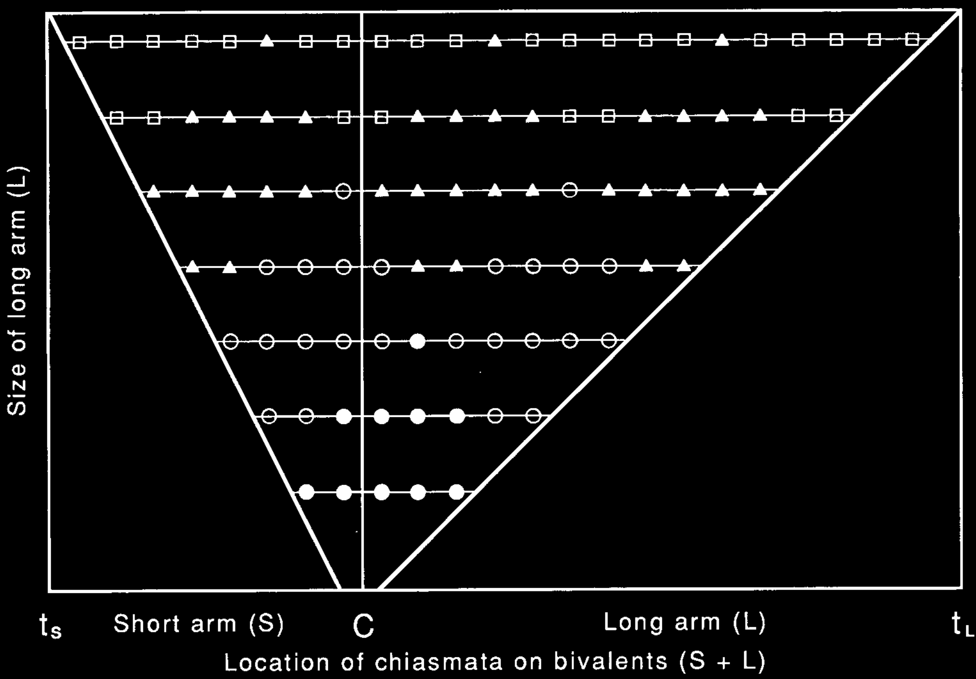

Fig. 4. Preliminary steps in construction of the chiasma distribution graph-(2). Chiasma distribution patterns of 1Xi (solid circles), 2Xi (open circles), 3Xi (solid triangles), and 4Xi (open squares) on bivalents of various sizes. It is assumed that the interstitial interference distance (*Ii*) is constant and is not interrupted by the centromere.

but interstitial chiasmata always distribute uniformly on the bivalents.

### *C. A general model for the chiasma distribution graph*

We consider in this section chiasma distribution graphs involving karyotypes with both acrocentrics (A) and metacentrics ($\overline{\text{M}}$). A and $\overline{\text{M}}$ chromosomes are euchromatic except for their pericentromeric heterochromatin and telomere regions.

Based on the definitions and references mentioned above, we assume in our model that the chiasma formation is inhibited in both the centromere region and the terminal region. These are denoted respectively as the minimum centromeric interference distance ($Ic_{\text{Min}}$) and the minimum terminal interference distance ($It_{\text{Min}}$) (Fig. 2b). $Ic_{\text{Min}}$ and $It_{\text{Min}}$ are indicated in Fig. 5 as gray zones. In Fig. 5, if the centromere interrupts the chiasma interference as suggested by Mather (1936, 1937), chiasma formation will occur independently in each arm (compare Figs 4 and 5). This means that the short and long arms of each bivalent are effectively equivalent to two independent telocentric chromosomes of size S or L.

The most generalized chiasma distribution graph is shown in Fig. 6, in which

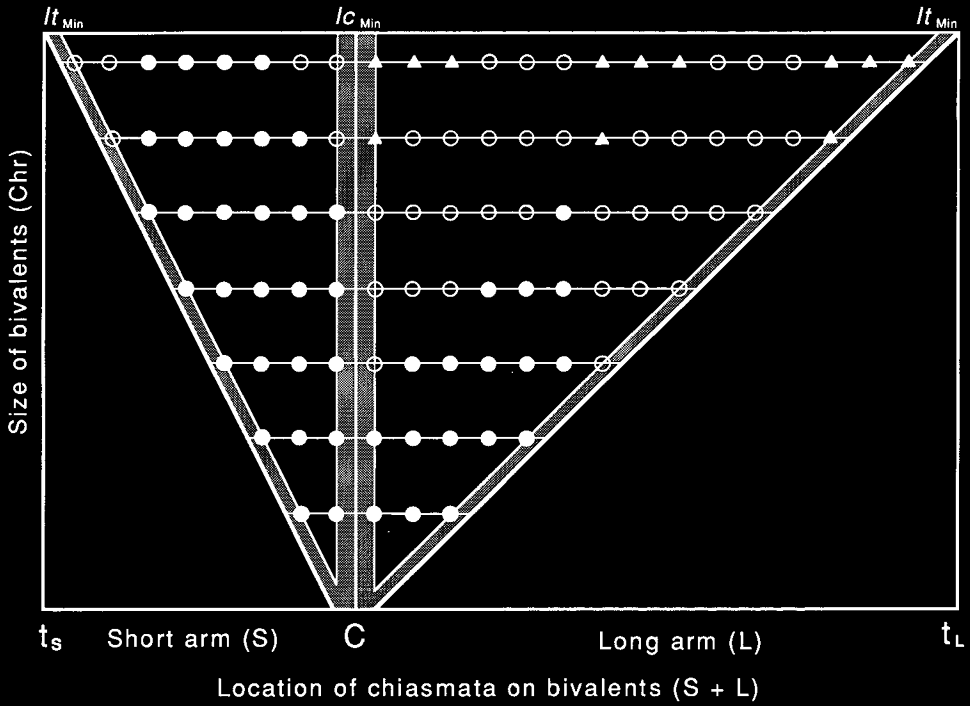

Fig. 5. Preliminary steps in construction of the chiasma distribution graph-(3). Distribution patterns of interstitial chiasmata (1Xi, 2Xi, 3Xi) on each bivalent, as expected by assuming the minimum centromeric interference distance ($Ic_{Min}$), the minimum terminal interference distance ($It_{Min}$) (gray zones), and that the centromere interrupts the transmission of chiasma interference, so that chiasma formation proceeds independently in each arm.

the ordinate indicates the size of arms (S or L) and the abscissa is the distance of chiasmata from the centromere on arms classified as (S or L). The distance between chiasmata and the centromere is estimated by the percent length relative to the total length of autosomal bivalents.

This chiasma distribution graph can be used to represent karyotypes of all kinds, including acrocentrics or metacentrics, or both. For example, the chiasma graph of Fig. 6 was derived from that of Fig. 5 by superimposing the short arms (dotted lines) on the long arms (solid lines). This graph is basically identical to that proposed by Imai and Moriwaki (1982; see their Fig. 8).

The chiasma distribution graph of Fig. 6 is also applicable where the centromere does not interrupt the chiasma interference. The chiasma graph in this case can be reconstructed from Fig. 4 by superimposing the short arms on the long arms with comparable size, though the distribution patterns of chiasmata are disordered in this case. We emphasize that the overall chiasma distribution is not affected by chiasma interference.

Note that the chiasmata are distributed uniformly on the short arms in both

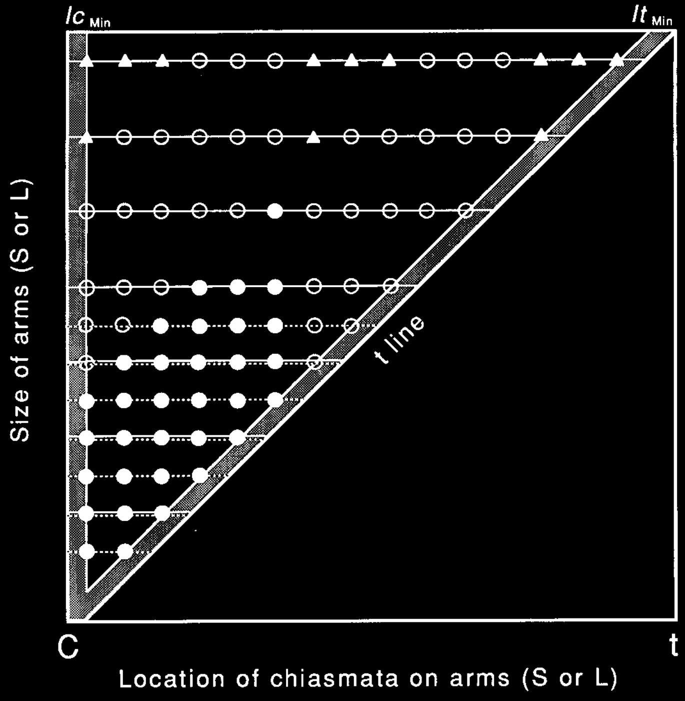

Fig. 6. A general model for the chiasma distribution graph, as applicable to karyotypes with metacentrics (M) or acrocentrics (A) or both. This graph was reconstructed from Fig. 5 by superimposing the short arms (dotted lines) on relevantly-sized long arms (solid lines).

Figs 4 and 5, and that the only difference between these figures relates to whether the chiasmata found in short (long) arms are recognized to be partners of those present in the relevant long (short) arms (Fig. 4), or considered to be independent from them (Fig. 5). In a qualitative sense it is difficult to discriminate the two in each case, but in a statistical sense such discrimination is possible. If the centromere inhibits chiasma formation but is not a barrier to chiasma interference, the chiasmata will distribute on some occasions around or across the centromere, except $lc_{\mathrm{Min}}$. Observed chiasma distribution patterns obviously do not support this expectation (e.g., Southern, 1967; Hulten, 1974; Jones, 1984; for further details see John, 1990).

## *D. The chiasma frequency graph*

In the chiasma distribution graph (Fig. 6), information about chiasma frequency is represented more or less qualitatively as a two-dimensional density distribution (Fig. 7a). To deal with this methodological limitation, we use the chiasma frequency graph (Fig. 7b). In this, the location of each chiasma is represented as a relative value on the standardized arm (S' or L' = 1.0), and the frequency of

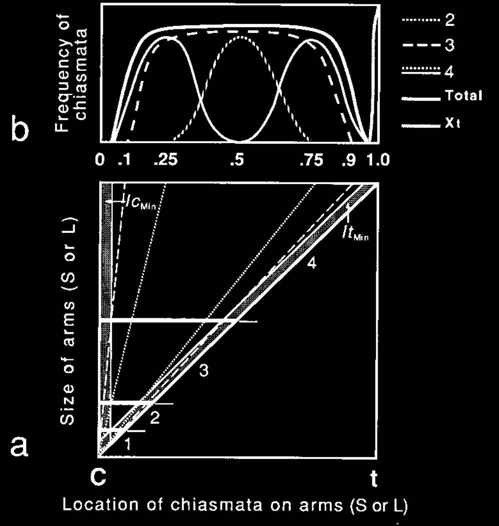

Fig. 7. Relationship between the chiasma distribution graph (a) and the chiasma frequency graph (b). The latter can be obtained from the former by standardizing all short (S) and long arms (L) at a value of 1.0 (i.e., S' or L'=1.0), and by estimating the gross chiasma frequency per 0.1 chiasma distance. Numerals indicate classes of arms (S or L) which are defined by $Ic_{\mathrm{Min}}$ and $It_{\mathrm{Min}}$; (1) (S or L)$<(Ic_{\mathrm{Min}}+It_{\mathrm{Min}})$, (2) $(Ic_{\mathrm{Min}}+It_{\mathrm{Min}})\leqq$(S or L)$<2(Ic_{\mathrm{Min}}+It_{\mathrm{Min}})$, (3) $2(Ic_{\mathrm{Min}}+It_{\mathrm{Min}})\leqq$(S or L)$<5(Ic_{\mathrm{Min}}+It_{\mathrm{Min}})$, and (4) $5(Ic_{\mathrm{Min}}+It_{\mathrm{Min}})\leqq$(S or L)$<10(Ic_{\mathrm{Min}}+It_{\mathrm{Min}})$. Xi distributions in each arm class in (a) show different Xi frequency distribution patterns in (b). Xt: terminal chiasma. C: centromere. t: terminal of arms. See text for details.

chiasmata is summed for each 0.1 unit length after rounding to two decimal places. Xc, Xi, and Xt are plotted on the graph at (S' or L')=0, 0<(S' or L')<1.0, and (S' or L')=1.0, respectively. As indicated above this method was used to analyze mouse chiasmata by Imai and Moriwaki (1982, see their Fig. 4).

If chiasmata are distributed uniformly on the chiasma distribution graph, an even frequency distribution would be theoretically expected in the chiasma frequency graph. The frequency distribution is effectively biassed by the standardization of the sizes of arms (S or L), and by the inhibition of chiasma formation in the centromere ($Ic_{\mathrm{Min}}$) and arm ends ($It_{\mathrm{Min}}$). Four major cases (1–4) are shown schematically in Fig. 7. They are characterized as follows:

(1) (S or L)$<(Ic_{\mathrm{Min}}+It_{\mathrm{Min}})$. Interstitial chiasmata are not detectable or are identified as terminal chiasma (Xt). Minute chromosomes and heterochromatic short arms of acrocentrics fall under this category.

(2) $(Ic_{\mathrm{Min}}+It_{\mathrm{Min}})\leqq$(S or L)$<2(Ic_{\mathrm{Min}}+It_{\mathrm{Min}})$. Only 1Xi bivalents appear in the middle sections of arms, which are represented in Fig. 7b as a normal curve distributing in 0.25≦(S' or L')≦0.75, and with a single peak at (S' or L')=0.5 (indicated as a dotted curve). This situation was termed "the centralization of chiasma distribution" by Imai and Moriwaki (1982).

(3) $2(Ic_{\mathrm{Min}}+It_{\mathrm{Min}})\leqq$(S or L)$<5(Ic_{\mathrm{Min}}+It_{\mathrm{Min}})$. 1Xi bivalents are dominant, but they distribute variously between 0.1≦(S' or L')≦0.9 in Fig. 7b (represented as a broken curve with a broad, flat peak).

(4) $5(Ic_{\mathrm{Min}}+It_{\mathrm{Min}})$ ≦(S or L)$<10(Ic_{\mathrm{Min}}+It_{\mathrm{Min}})$. Both 1Xi and 2Xi bivalents will appear if $Ii$ is approximately $5(Ic_{\mathrm{Min}}+It_{\mathrm{Min}})$. 1Xi bivalents distribute in 0.25≦(S' or L')≦0.75 as in case (2) above, but here the 2Xi bivalents have bimodal distribution, with two peaks near the values 0.25 and 0.75 in Fig. 7b (represented

as a thin unbroken curve).

Note that the three frequency distribution curves discussed above counterbalance each other in Fig. 7b, and the chiasma frequency per unit length thus becomes almost uniform or constant in the area $0.1 \leqq (S' \text{ or } L') \leqq 0.9$ (represented as a thickly-lined curve). In contrast to interstitial chiasmata, the frequency of the terminal chiasma (Xt) is always plotted at $(S' \text{ or } L')=1.0$ in Fig. 7b (represented as a meshed curve).

In short, if chiasma formation is a random event, the interstitial chiasmata distribute uniformly on the arms in the chiasma distribution graph, except for the centromeric and telomeric areas. The frequency distribution pattern of interstitial chiasmata will be methodologically biassed in the chiasma frequency graph by the centralization of chiasma distribution. This bias will be most notable in small-sized arms with $(S \text{ or } L) < 2(Ic_{\mathrm{Min}} + It_{\mathrm{Min}})$. We emphasize, however, that the same problem is inherent in the conventional histogram method.

Finally, we note the effect of constitutive heterochromatin (C-bands) in chiasma graphs. It is well documented that chiasma formation is inhibited in chromosomal sections including constitutive heterochromatin (e.g., Miklos and Nankivell, 1976; Yamamoto and Miklos, 1978; for more details see John and Miklos, 1979, and Sumner, 1990). Thus, the heterochromatic regions of C-banded chromosomes ($A^{M}$, $A^{c}$, $A^{i}$, $A^{t}$, $\overline{M}^{i}$, $\overline{M}^{t}$ or $\overline{M}^{tt}$) are represented on the chiasma distribution graph as blank areas with regard to chiasma distribution (for definitions of chromosome morphologies see Imai, 1991). In those cases involving totally heterochromatic arms of acrocentrics (A) or pseudoacrocentrics ($A^{M}$), only terminal chiasmata (Xt) would be plotted on the t line at their relevant arm size (S or L).

## 5. OBSERVATIONS

### A. *Chiasma analyses of male Chinese hamster*

*Pseudochiasmata at early diplotene*: Because the sizes of bivalents contract gradually during meiosis I, two perplexing problems arise in chiasma analyses (Fig. 8). They involve the presence of pseudochiasmata in early diplotene, and pseudoterminalization of interstitial chiasmata in late metaphase I. The former results from twisting of elongated bivalents (Figs 1-(2) and 8a), and causes overestimation of chiasma frequency per cell (FXi). Conversely, FXi is underestimated where pseudoterminalization of interstitial chiasmata is present at late metaphase I. We have attempted to estimate the bias due to pseudochiasmata by using the interstitial interference distance ($Ii$), because $Ii$ values will decrease by pseudochiasmata.

We investigated $Ii$ at various cell stages of meiosis I, with the results that $Ii = 2.58(\%) \pm 1.68$ (s.d.) at early diplotene, 6.84±3.05 (late diplotene), 7.21±3.05 (diakinesis), 7.64±2.74 (early metaphase I), and 8.14±2.58 (late metaphase I). Because the $Ii$ value is significantly lower at early diplotene than at other stages,

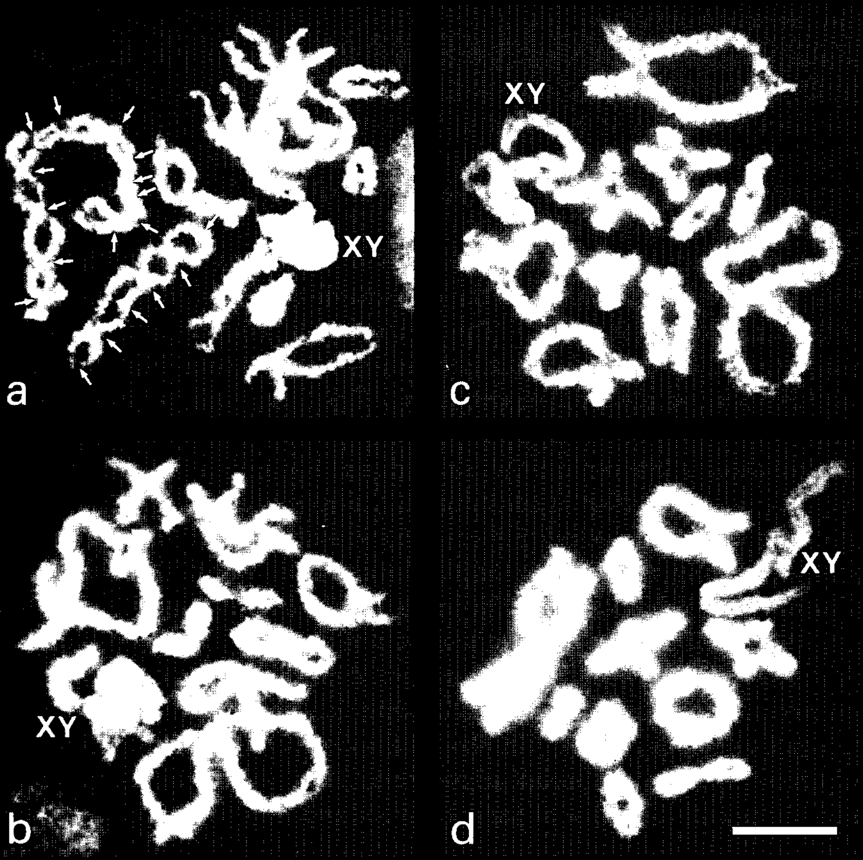

Fig. 8. Meiotic figures at early diplotene (a), late diplotene (b), diakinesis (c), and early metaphase I (d). Small arrows in (a) indicate apparent interstitial chiasmata which are in fact artificial, resulting from the twisting of bivalents. XY: Sex chromosomes. Bar represents 5 μm.

we conclude that most pseudochiasmata disappear before late diplotene in the Chinese hamster. The slight increase in the value of *Ii* in late metaphase I is due mainly to continuous contraction of bivalents. For this reason, we use the bivalents obtained from late diplotene (Fig. 8b), diakinesis (Fig. 8c), and early metaphase I (Fig. 8d) for detailed chiasma analyses. To simplify terminology, the words diplotene and metaphase I are used instead of late diplotene and early metaphase I.

*Dissociation of terminal chiasmata (Xt) during diakinesis and metaphase I*: The bivalents of Chinese hamsters are classified in our analysis into three major classes, mXi.2Xt, mXi.1Xt and mXi, where $0 \leq m \leq 5$. Their frequencies at diplotene (DP), diakinesis (DK), and metaphase I (MI) vary as follows: 1.6% → 0.3

→ 0.3 in mXi.2Xt, 24.8% → 23.1 → 16.6 in mXi.1Xt, and 73.6% → 76.6 → 83.1 in mXi. The gross frequencies of mXi.2Xt and mXi.1Xt bivalents decrease gradually during DK and MI (−1.3+(−8.2)=−9.5%), while those of mXi bivalents increase alternatively (+9.5%). These results do not support the chiasma terminalization hypothesis, because if interstitial chiasmata (Xi) move to termini, the frequencies of mXi should decrease at DK and MI (e.g., mXi → (m-1)Xi.1Xt → (m-2)Xi.2Xt). The alternative is to assume continuing dissociation of terminal chiasmata (mXi.2Xt or mXi.1Xt → mXi) through DK and MI. The dissociation of Xt can be visually demonstrated using the chiasma graph method.

*Chiasma distribution patterns on the chiasma distribution graph*: Because most pseudochiasmata disappear during diplotene, and contraction of bivalents is less prominent at diakinesis than at metaphase I, we use bivalents at diakinesis for the chiasma distribution graph. The chiasma distribution graph for Chinese hamsters is shown in Fig. 9. The results of this analysis are summarized as follows:

(1) The minimum centromeric interference distance ($Ic_{\mathrm{Min}}$) and the minimum terminal interference distance ($It_{\mathrm{Min}}$) are constant, i.e., $Ic_{\mathrm{Min}}=It_{\mathrm{Min}}=0.5$, in arms

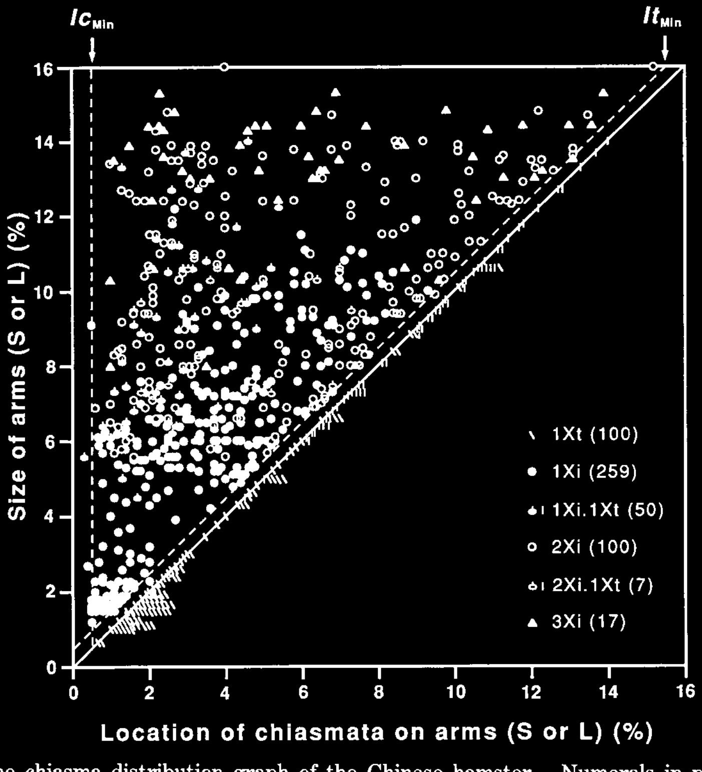

Fig. 9. The chiasma distribution graph of the Chinese hamster. Numerals in parentheses are total numbers of each relevant bivalent type.

of all sizes (represented as broken lines in Fig. 9).

(2) The size of arms (S or L) ranges between 1.0 and 16.0, and interstitial chiasmata (1Xi, 2Xi, and 3Xi) are distributed in general randomly and almost uniformly on the arms, except for $Ic_{\text{Min}}$ and $It_{\text{Min}}$. (The gap in chiasma distribution in $3 \leqq (\text{S or L}) \leqq 5$ is due to a lack of relevant-sized arms in Chinese hamster karyotype).

(3) The 1Xi, 2Xi, and 3Xi chiasmata appear in arms with $1.0 \leqq (\text{S or L}) \leqq 12$, $5 \leqq (\text{S or L}) \leqq 16$, and $10 \leqq (\text{S or L}) \leqq 16$, respectively. Although their distributions overlap rather broadly, the chiasma frequencies per arm (FX/b) are roughly proportional to the sizes of the arms (S or L).

*Fluctuation of the interstitial interference distance (Ii)*: As pointed out in (3) above, the 1Xi and 2Xi arms overlap in $5 \leqq (\text{S or L}) \leqq 12$ (Fig. 9). In this zone, two chiasmata on 2Xi arms tend to be distributed separately in distal and proximal areas (open circles). Alternatively, the single chiasma of the 1Xi arms (solid circles) intercalates between them. These mosaic patterns seem partly consistent with that illustrated in Figs 6 and 7 (case 4), but they are not always as clear-cut as would be theoretically expected. One reason for this might be fluctuation of the interference distance (*Ii*) which was assumed as constant by Mather (1937).

To test this possibility, we examined the *Ii* values derived from 2Xi and 3Xi

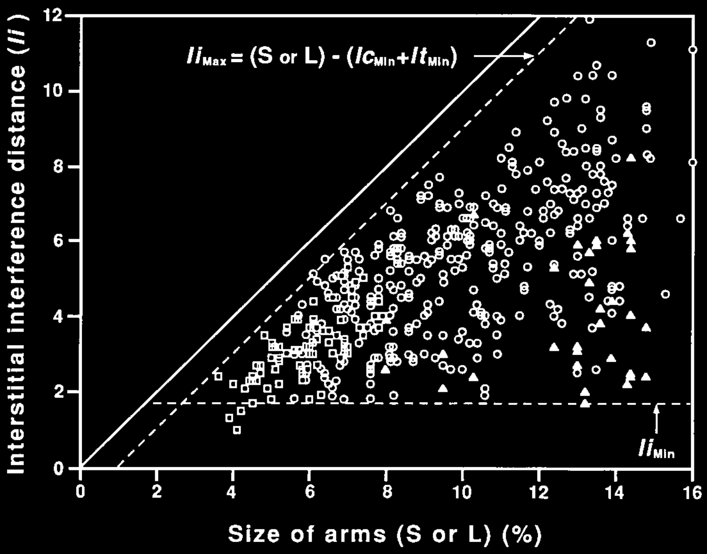

Fig. 10. Correlation between the interstitial interference distance (*Ii*) and arm size (S or L) in the Chinese hamster (open circles for 2Xi and solid triangles for 3Xi) and BALB/c mice (open squares for 2Xi). $Ii_{\text{Min}}=1.8\%$ (of total bivalent length at diakinesis). $Ii_{\text{Max}}=(\text{S or L})-(Ic_{\text{Min}}+It_{\text{Min}})=(\text{S or L})-1.0\%$. Note that the *Ii* values are not constant but fluctuates almost randomly between $Ii_{\text{Max}}$ and $Ii_{\text{Min}}$.

arms of various sizes. The result is really surprising. $Ii$ values proved not to be constant at all, but to fluctuate remarkably (Fig. 10). There is a tendency for the mean $Ii$ values in 2Xi arms (open circles in Fig. 10) to increase linearly with increase in arm size. For example, $Ii=3.9\pm1.1$ in $5<(\mathrm{S}\text{ or }\mathrm{L})<8.0$, $Ii=5.7\pm1.6$ in $10.0\leqq(\mathrm{S}\text{ or }\mathrm{L})<12.0$, and $Ii=7.7\pm2.3$ in $14.0\leqq(\mathrm{S}\text{ or }\mathrm{L})\leqq16.0$. On the other hand, $Ii$ values of 3Xi arms are significantly lower ($Ii=3.4\pm1.5\sim4.3\pm2.1$ in $8\leqq(\mathrm{S}$ or L); solid triangles in Fig. 10) than those of 2Xi.

The distribution patterns of $Ii$ values in Fig. 10 indicate that the interstitial interference distance fluctuates randomly between the minimum interstitial interference distance ($Ii_{\mathrm{Min}}$) and the maximum interstitial interference distance ($Ii_{\mathrm{Max}}$). In Chinese hamster, $Ii_{\mathrm{Min}}=1.8$ and $Ii_{\mathrm{Max}}=(\mathrm{S}\text{ or }\mathrm{L})-(Ic_{\mathrm{Min}}+It_{\mathrm{Min}})=(\mathrm{S}\text{ or }\mathrm{L})-1.0$ (broken lines in Fig. 10).

The evidence that $Ii$ values are smaller in 3Xi arms than in 2Xi arms may be stochastically interpretable as follows: in a large sized arm, if two closely-located interstitial chiasmata (i.e., low $Ii$ values) occurred by chance, the probability that a third will occur increases with increasing arm length. The same is true for 2Xi versus 1Xi.

*Chiasma frequency distributions on standardized arms*: We have examined the gross frequency distributions of chiasmata on standardized arms (S' or L')=1.0 at diplotene, diakinesis, and metaphase I (Fig. 11). Major results and interpreta-

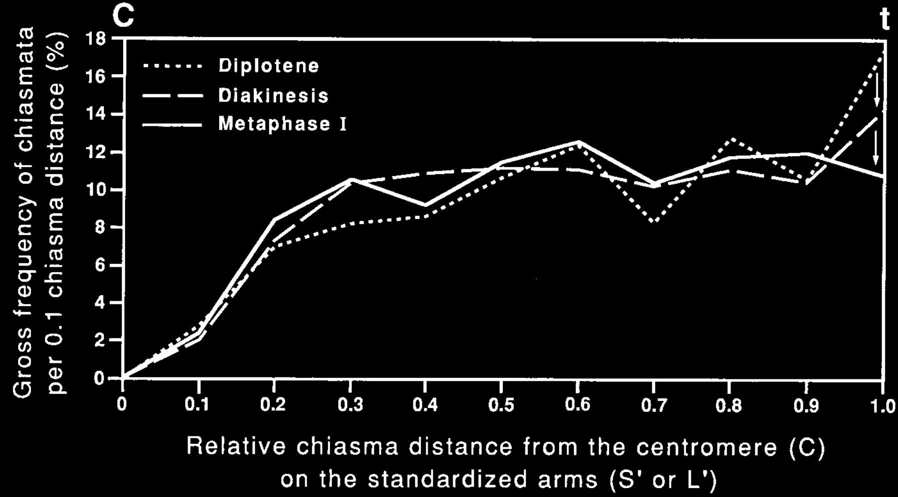

Fig. 11. The chiasma frequency graph of the Chinese hamster at diplotene, diakinesis, and metaphase I. Note that chiasma frequency is roughly constant in the area $0.2\leqq(\mathrm{S'}$ or $\mathrm{L'})\leqq0.9$, indicating that interstitial chiasmata (Xi) distribute randomly and uniformly on bivalents except for $Ic_{\mathrm{Min}}$ and $It_{\mathrm{Min}}$, and that there is no chiasma terminalization. The gradual decrease of Xt frequency at (S' or L')=1.0 results mostly from dissociation of the achiasmatic terminal association (see Fig. 1-(4)).

tions are:

(1) The gross frequency of interstitial chiasmata (Xi) is extremely low (ca. 2%) in the range (S' or L')$\leqq 0.1$ in all three cell stages.

(2) The gross frequency of Xi is roughly constant ($10 \pm 2\%$) in the ranges $0.2 \leqq$(S' or L')$\leqq 0.9$ in all three cell stages.

(3) The gross frequency of terminal chiasmata (Xt) at (S' or L')$=1.0$ is 17.5% at diplotene, but decreases continuously through diakinesis (14.3%) and metaphase I (10.8%) (see arrows in Fig. 11).

Item (1) results from the centromeric interference distance ($Ic$). Item (2) corresponds to the random and uniform distribution of Xi in Fig. 9. The even frequency distributions of Xi at DP, DK, and MI indicates strongly that chiasma terminalization does not occur in Chinese hamsters. Item (3) is interpreted as being due to the dissociation of Xt through achiasmatic terminal association, as mentioned above.

*Chiasma frequency per cell (FX)*: We have examined two categories of chiasma frequency per cell, FXit and FXi, at diplotene (DT), diakinesis (DK), and metaphase I (MI). The results are $\mathrm{FXit_{DP}}=19.3 \pm 1.8$, $\mathrm{FXit_{DK}}=18.3 \pm 1.5$, and $\mathrm{FXit_{MI}}=17.5 \pm 1.2$, while $\mathrm{FXi_{DP}}=16.4+1.2$, $\mathrm{FXi_{DK}}=15.7+1.2$, and $\mathrm{FXi_{MI}}=15.7 \pm 1.2$.

There is a gradual decrease in both FXit and FXi values (ca. $-1 \sim -2$) at diakinesis and metaphase I. Conventionally this has been held to provide evidence supporting chiasma terminalization. We propose an alternative possibility for the FXi case, namely dissociation of the achiasmatic terminal association (Xt).

It is also noteworthy that FXit values are slightly but significantly (ca. $+2 \sim +3$) higher than FXi values in each cell stage. Although this is not especially prominent in Chinese hamsters, it will be shown below to be noteworthy in mice and dogs.

### *B. Chiasma analyses of male BALB/c mice*

We have reexamined the original BALB/c mouse data of Imai and Moriwaki (1982) using the chiasma distribution graph method (Fig. 12). The major results and comments are as follows;

(1) The size of bivalents ranges $2<$(S or L)$<8$. Because the karyotype of mice comprises only acrocentric chromosomes ($K=20A$) and as the size of relevant short arms (S) is negligibly small, the arms (whether considered S or L) are in practical terms all long (L).

(2) The interstitial chiasmata of 1Xi and 2Xi bivalents generally distribute randomly and uniformly between $Ic_{\mathrm{Min}}=0.6$ and $It_{\mathrm{Min}}=0.6$ in Fig. 12. This pattern is almost comparable to that of Chinese hamsters (Fig. 9).

(3) The interstitial interference distance of BALB/c mice (as well as Chinese hamsters) fluctuates randomly between $Ii_{\mathrm{Min}}=1.8$ and $Ii_{\mathrm{Max}}=$(S or L)

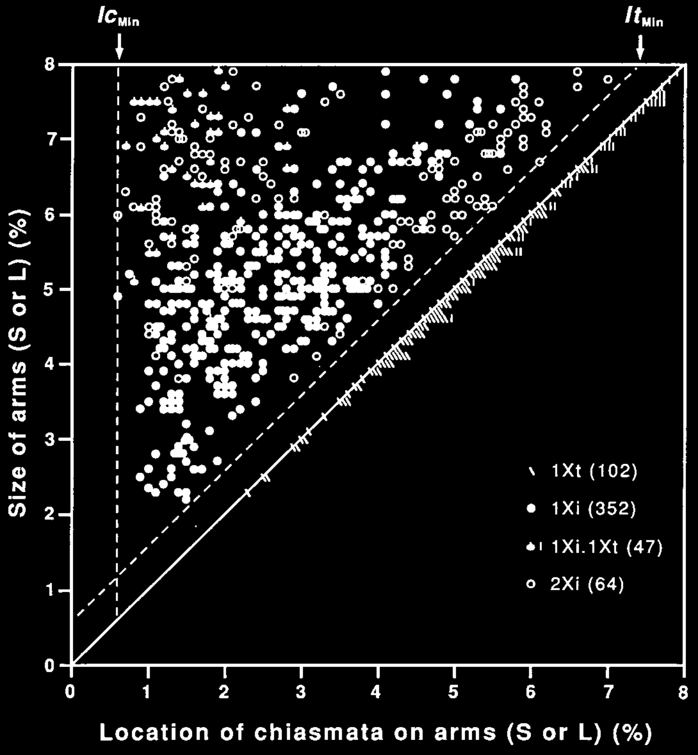

Fig. 12. The chiasma distribution graph of BALB/c mice. Numerals in parentheses are total numbers of each relevant bivalent type.

$-(Ic_{\text{Min}}+It_{\text{Min}})=(\text{S or L})-1.0$ (open squares in Fig. 10).

(4) 2Xi chiasmata appear in arms with (S or L)$\geqq$3.8, and they show a bimodal frequency distribution with one peaks in the proximal and distal regions.

(5) 1Xi arms distribute in 2<(S or L)<8. They appear predominantly in bivalents with (S or L)<5, and the distribution of 1Xi intercalates the bimodal frequency distribution of 2Xi in the arm range 5<(S or L)<8.

(6) 1Xt arms predominate in small-sized bivalents with (S or L)<6. On the other hand, 1Xi.1Xt arms appear in large-sized bivalents with (S or L)>5.5.

Further information of chiasmata may be obtained from the chiasma frequency graph, as follows (Fig. 13):

(7) The interstitial chiasmata (Xi) show a unimodal distribution with a broad, flat peak in the range 0.4$\leqq$(S' or L')$\leqq$0.7 (ca. 12±1.0%). This frequency pattern is quite different from that of Chinese hamsters (Fig. 11), but is consistent with that expected theoretically in Fig. 7 (see case 3). In other words, the remarkable reduction of chiasma frequencies indicated in (S' or L')$\leqq$0.2 and 0.8$\leqq$(S' or L')$\leqq$0.9 in mice is due mostly to the methodological characteristics of the chiasma

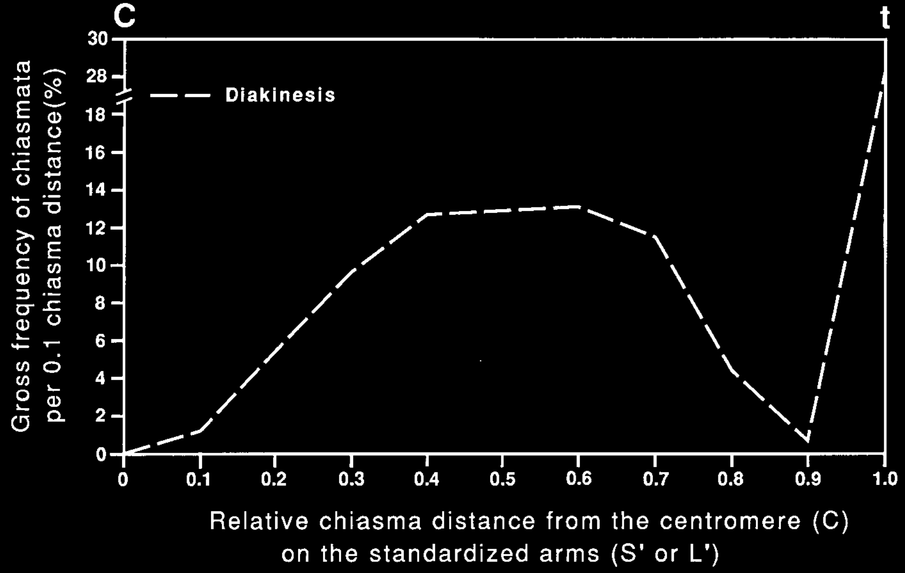

Fig. 13. The chiasma frequency graph of BALB/c mice. The Xi frequency shows a unimodal distribution, with a broad, flat peak in the range $0.4 \leqq (S' \text{ or } L') \leqq 0.7$. The remarkable reduction of chiasma frequency in $(S' \text{ or } L') \leqq 0.2$ and $0.8 \leqq (S' \text{ or } L') \leqq 0.9$ is due mostly to inhibition of chiasma formation at centromere and telomere ($Ic_{\text{Min}} = It_{\text{Min}} = 0.6$, see Fig. 12).

frequency graph. Note that as $Ic_{\text{Min}} = It_{\text{Min}} = 0.6$, the arm-size required to satisfy case 3 in Fig. 7, i.e., $2(Ic_{\text{Min}} + It_{\text{Min}}) \leqq (S \text{ or } L) < 5(Ic_{\text{Min}} + It_{\text{Min}})$, is estimated to be $2.4 < (S \text{ or } L) < 6$, which is almost comparable to the observations reported here in the range $2 < (S \text{ or } L) < 8$ (Fig. 12).

(8) The frequency of terminal chiasmata (Xt) at $(S' \text{ or } L') = 1.0$ (including $Xt_S$ of 2Xt bivalents) is more than twice (28.5%) that of Xi (12%) in the range $0.4 \leqq (S' \text{ or } L') \leqq 0.7$. Since the practical range of Xt values is 0.05 (i.e., S' or L'=0.95~1.0), the revised Xt value per 0.1 unit length is $28.5 \times 2 = 57.0$, i.e., the frequency of Xt is 4.8 times higher than that of Xi. This result is inconsistent with the origin of Xt by pseudoterminalization, but is simply interpretable by assuming Xt by achiasmatic terminal association.

(9) According to Imai and Moriwaki (1982), $FXit_{DK} = 23.1 \pm 1.7$ and $FXi_{DK} = 17.1 \pm 2.3$. The FXit value is significantly higher (+6) than the FXi value.

## *C. Chiasma analyses of domestic dogs*

Although available data for dogs is not yet sufficient for detailed analysis, some noteworthy information is available on relevant chiasma distribution patterns (Fig. 14). These are itemized as follows:

(1) Since the chromosome number of dogs is high $2n = 78$ $(n = 39)$, average arm

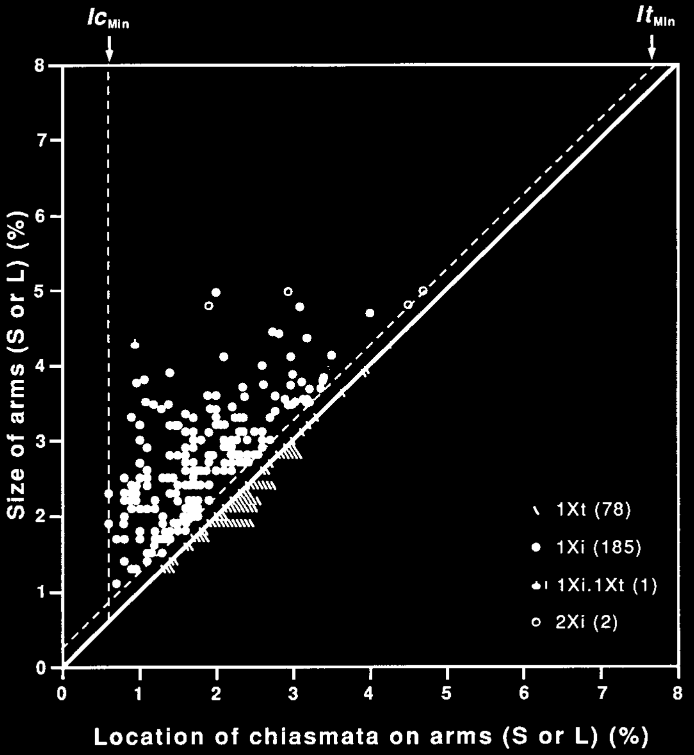

Fig. 14. The chiasma distribution graph of the domestic dog. $Ic_{Min}=0.6$ and $It_{Min}=0.25$.

size is much smaller, $1<(S \text{ or } L)<3.5$, than in mice ($n=20$; $2<(S \text{ or } L)<8$) or Chinese hamsters ($n=11$; $1<(S \text{ or } L)<16$).

(2) $Ic_{Min}=0.6$ but $It_{Min}=0.25$. The latter is low compared to that for the Chinese hamster ($It_{Min}=0.5$) or mice ($It_{Min}=0.6$). This is simply explained: the accuracy of chiasma detection in our system depends mostly on the width of chromatin present ($W_b$, or more precisely $(2/3)W_b$). As $W_b$ equals 0.4 in domestic dogs, 0.8 in Chinese hamsters, and 0.9 in mice, $(2/3)W_b=0.27$, 0.5, and 0.6, respectively. Thus, the bivalents of dogs are significantly more slender than those of hamsters or mice.

(3) Because the size of arms is small, only 1Xi and 1Xt chiasmata were observed.

(4) The interstitial chiasmata (Xi) scatter on the arms somewhat randomly, except for $Ic_{Min}$ and $It_{Min}$.

(5) $FXit_{DK}=42.6\pm2.4$ and $FXi_{DK}=27.1\pm3.0$. Although relevant values are preliminary, that for FXit is conspicuously higher (+15.5) than that of FXi.

## 6. DISCUSSION

The chiasma (X) has been investigated above from historical, theoretical, and experimental points-of-view. A fundamental conclusion here is that, despite other techniques, optically perceived chiasma still provides effective cytological information for the analysis of crossing-over.

Chiasmata have at least two separate biological functions: gene shuffling, and the binding of bivalents in meiosis I. When they are divided into interstitial (Xi) and terminal (Xt) types, Xis contribute both to gene shuffling and to the binding bivalents. Xts, however, serve only to bind the termini of bivalents. These Xi and Xt categories have been confused in classical cytogenetics. Since our arguments are centered on gene shuffling, the distribution of Xi on bivalents and the frequency of interstitial chiasmata per cell (FXi) are emphasized in this paper.

However, matters are not so simple, in that FXi values would be biassed if Xi chiasmata move terminally and become Xt through chiasma terminalization, or if Xi chiasmata present in subterminal regions are identified as Xt by pseudoterminalization. Our opinions regarding terminal chiasmata will now be reviewed, followed by discussion of some statistical characteristics of Xi chiasmata based on our experimental data. Finally we will consider the cytological significance of chiasma frequency.

### A. *New aspects regarding terminal chiasma (Xt)*

The expression "terminal chiasma" has been applied broadly to cover the so-called end-to-end association of bivalents. At least four relevant entities have been involved or are theoretically possible: (1) terminal chiasma in the literal meaning of the term, (2) Xi chiasmata which have moved to chromosome ends by chiasma terminalization, (3) Xi chiasmata which are present in subterminal regions but misidentified as Xt due to pseudoterminalization, and (4) an achiasmatic terminal association of bivalents. Details and discussion follow:

*(1) The terminal chiasma, in the literal meaning of the term:* This category is applicable to chiasmata present at the actual termini of bivalents. If these occur in nature, recombination nodules (RNs) should appear at the basal knob or on the nuclear membrane at pachytene. This possibility seems unlikely, because the majority of RNs distribute somewhat proximally to the basal knob in autosomal bivalents, e.g., fungi (*Sordaria macrospora*; Zickler, 1977), humans (Solari, 1988), silkworms (*Bombyx mori*; Holm and Rasmussen, 1980), wheat var. Chinese Spring (Hobolth, 1981) - for further details see Wettstein (1984).

It is also noteworthy that the frequency of recombination per unit length of DNA is reduced near the centromere and telomeres in *Drosophila melanogaster* (Charles, 1938; Lindsley and Sandler, 1977; Morton et al., 1976). These data imply that chiasma formation is inhibited in the subterminal regions of autosomal bivalents as well as in the region of the centromere, i.e., in our terms $Ic_{\mathrm{Min}}$ and $It_{\mathrm{Min}}$.

*(2) Xt by terminalization of Xi:* As indicated above, chiasma terminalization as posited by Darlington (1932) should now be considered obsolete, following the BrdU labeling experiments of Tease and Jones (1978) and Kanda and Kato (1980). Our work on Chinese hamster supports this conclusion (Fig. 11). If a species with chiasma terminalization were to be discovered, this would mean simply that the species is one unsuitable for chiasma analysis.

*(3) Xt by pseudoterminalization of Xi:* The pseudoterminalization of interstitial chiasmata depends mostly on the contraction of bivalents and the accuracy of the measurement, which is roughly determined by the width of chromatin in half bivalents ($W_b$).

In enlarged photographs (×4,500–6,500), $W_b$ value compared to the total length of autosomal bivalents at diakinesis is 0.8 in Chinese hamster, 0.9 in BALB/c mice, and 0.4 in domestic dogs. On the other hand, the most terminal Xi detected by us are about 2/3 the width of relevant half bivalents ($W_b$), i.e., $(2/3)W_b=0.5$, 0.6, and 0.26, respectively. This means that Xi chiasmata which occurred within $(2/3)W_b$ of the termini would be detected as Xt. This situation is visually represented as the minimum terminal interference distance ($It_{\mathrm{Min}}$) in the chiasma distribution graph (Figs 9, 12, 14), where $It_{\mathrm{Min}}=0.5$ in Chinese hamster, 0.6 in mice, and 0.25 in dogs. Thus, $It_{\mathrm{Min}}=(2/3)W_b$. This does not mean, however, that all recognized terminal chiasmata result from misidentification of subterminal interstitial chiasmata. There are at least two possible mechanisms for $It_{\mathrm{Min}}$, namely: inhibition of chiasma formation near the ends of bivalents, as discussed in (1) above, and achiasmatic terminal association, which will now be discussed.

*(4) Achiasmatic terminal association:* In this association the basal knob-nuclear membrane structure is complex (Fig. 1). It was recently termed "telochore" by Suja and Rufas (1994). This structure appears at pachytene (Wettstein, 1984; Moens and Pearlman, 1990) and degenerates during diplotene (Solari, 1970). There is, however, evidence indicating that the telochore remains during diplotene as remnant fragments in some autosomal bivalents (Solari, 1970; Tres, 1977; Goetz et al., 1984). The terminal association seems to be fragile or unstable when examined: it readily dissociates, either because of increasing stiffness of bivalents due to contraction of chromatin, or hypotonic treatment. Dissociation of Xt was observed by us in Chinese hamster: the frequency of Xt was reduced gradually in diakinesis and metaphase I (Fig. 11, see arrows).

The fact that no recombination nodules have been observed on the basal knob or nuclear membrane, as mentioned under (1) above, is consistent with the achiasmatic terminal association. If chiasma formation proceeds on the synaptonemal complex by the transformation of relatively flexible recombination nodules to chromatin nodules with a more rigid structure (see Fig. 12 in the text by Rasmussen and Holm, 1984), Xt chiasmata resulting from pseudoterminalization would not dissociate at diakinesis and metaphase I.

There is indisputable evidence that in humans and mice, the so-called end-to-end association of the sex chromosomes, which occurs at the pseudoautosomal region, is chiasmatic (e.g., Evans et al., 1982; Glamann, 1986; Rouyer et al., 1986; Solari, 1988-for further details see Solari, 1994). We exclude such obligate crossing-overs from the view point of gene shuffling, because the recombining pseudoautosomal region is mostly noncoding and only one or two genes are involved-for example, *MIC2* and *CSF2R* in humans (Brown, 1988; Petit et al., 1988), and *Sts* in mice (Keitges et al., 1985). If obligate crossing-over is a mechanism for binding the X and Y chromosomes, it would not be inconsistent for the achiasmatic terminal association to assume a "double lock"-involving obligate crossing-over at the pseudoautosomal region, and achiasmatic terminal association in the vicinity of the telochore. Figures 68, 78A and 79 of Solari (1994) suggests such a possibility. The achiasmatic terminal association is not known to operate in mice and humans, but might have played a significant role in *Microtus agrestis* (Wolf et al., 1988; Ashley et al., 1989), *Rattus norvegicus* (Joseph and Chandley, 1984), and *Psammomys obsess* (Solari and Ashley, 1977).

In short, we cannot exclude Xt by pseudoterminalization of subterminal Xi from consideration, but most Xt chiasmata at diakinesis are achiasmatic terminal associations.

### *B. Statistical characteristics of the interstitial chiasma (Xi)*

Mather (1936, 1937) recognized two classes of chiasma distance: differential distance (between the centromere and the first proximal chiasma; *Ic* in our terminology) and interference distance (between two interstitial chiasmata; *Ii* in our terminology). He assumed that the differential distance is variable in bivalents, but that interference distance is constant within and between bivalents.

Our results are contrary: they suggest that chiasma formation is principally a random event, but that there is partial inhibition of chiasma formation in $Ic_{\mathrm{Min}}$, $It_{\mathrm{Min}}$ and $Ii_{\mathrm{Min}}$. When three classes of interference distance are recognized, namely: centromeric interference distance (*Ic*), interstitial interference distance (*Ii*), and terminal interference distance (*It*), our results indicate that: (1) there is a minimum centromeric interference distance ($Ic_{\mathrm{Min}}$), which is constant ($Ic_{\mathrm{Min}}=0.5$–$0.6$) for arms of all sizes (S or L) in Chinese hamsters, mice and dogs (Figs 9, 12, and 14). (2) *Ii* values fluctuate almost randomly between the minimum interstitial interference distance ($Ii_{\mathrm{Min}}=1.8$) and the maximum interstitial interference distance ($Ii_{\mathrm{Max}}=(\mathrm{S}\text{ or }\mathrm{L})-(Ic_{\mathrm{Min}}+It_{\mathrm{Min}})$) (Fig. 10). And (3) the distribution of interstitial chiasmata on 1Xi bivalents are also random and uniform between $Ic_{\mathrm{Min}}$

and $It_{\mathrm{Min}}$ (see solid circles in Figs 9, 12, and 14).

There are some species in which chiasmata localize either only proximally (e.g., *Trillium kamtschaticum*, Jones, 1974; *Stethophyma grossum*, John, 1990) or only distally (*Aedes aegypti*, Ved Brat and Rai, 1973). We are inclined to consider that these species, along with male *Drosophila melanogaster* (which lack chiasmata) and male ants (which have no meiotic division due to male haploidy) might be special cases derived secondarily from the original random distribution system. Although it is important to investigate chiasma formation in these and other exceptional systems, our major aim in this paper is to construct a general model enabling a statistical description of chiasma phenomena. The most important achievement of our approach is the demonstration that these random event are easily estimated theoretically.

With regard to the initiation site of chiasmata, Mather (1937) assumed that chiasma formation proceeds from centromere to telomere, with a constant interval occasioned by the interference distance. An alternative course, from telomere to centromere, was proposed by Fox (1973). We propose a third possible alternative based on random processes. In our model a group of recombination nodules (RNs) attach at random to the synaptonemal complex (SC), except for the areas designated $Ic$ and $It$, and transmit interference signals in both directions, just as in the fertilization wave. If other RNs were to arrive at the SC after the interference signal has passed, they would be removed as abortive. If there is no interference signal, $Ii_{\mathrm{Min}}$ values would be far less than 1.8, because the accuracy of chiasma observations in our investigations is $0.26 \sim 0.6$ $(=It_{\mathrm{Min}})$.

If interference signals proceed in both directions, one recombination nodule would inhibit chiasma formation in the areas $1Ii_{\mathrm{Min}} \sim 2Ii_{\mathrm{Min}}$ and the process would also be inhibited in $Ic_{\mathrm{Min}}$ and $It_{\mathrm{Min}}$. Therefore, 2Xi chiasmata will not appear in small arms with (S or L)$\leqq(1 \sim 2)Ii_{\mathrm{Min}} + Ic_{\mathrm{Min}} + It_{\mathrm{Min}} = 2.8 \sim 4.8$ in Chinese hamsters and mice. On the other hand, the smallest 2Xi bivalents observed in these animals have (S or L)$=3.8 \sim 5.6$ and these values are close to the theoretical expectation.

The interpretations indicated above are consistent with the polymerization model of chiasma interference proposed by King and Mortimer (1990). These authors concluded that early RNs bind randomly to the SC and that some of them initiate polymerization reactions. The growing polymers (corresponding to our interference signal) reject other RNs.

A somewhat different model, "chiasma interference as a function of genetic distance", was proposed by Foss et al. (1993). In this, recombination-initiation events occur at random, following a Poisson distribution. The frequency distribution patterns of 1Xi, 2Xi, and 3Xi chiasmata estimated by Lande and Stahl (1993) seems to be compatible with our conclusions (see case 4 in Fig. 7; $5(Ic_{\mathrm{Min}} + It_{\mathrm{Min}}) \leqq$ (S or L) $< 10(Ic_{\mathrm{Min}} + It_{\mathrm{Min}})$). We are, however, not convinced that the model can interpret the $Ii_{\mathrm{Min}}$ value recorded in our work (Fig. 10).

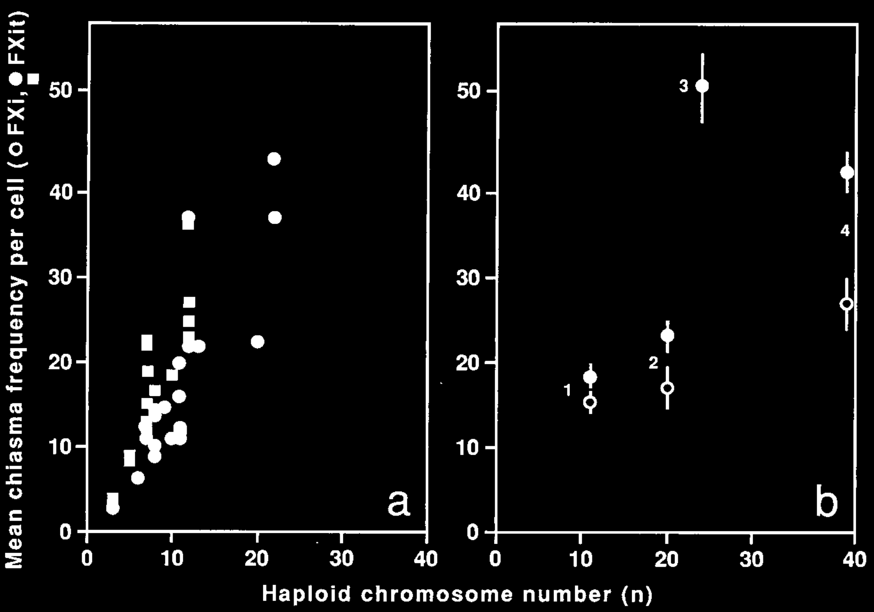

Fig. 15. A positive correlation between mean chiasma frequencies per cell (FXit, solid circles for animals and solid squares for plants) and haploid chromosome number (n) reported in eukaryotes (a), and comparison of FXi (open circles) and FXit (solid circles) values of Chinese hamster (1), BALB/c mice (2), and dogs (4) (b). We demonstrate in this paper that FXit values are grossly overestimated relative to FXi values, especially in species with n≧20. This results from different assumptions regarding the cytological meaning of terminal chiasma (Xt). Note that FXit includes terminal chiasmata (Xt), but FXi excludes Xt, because Xt chiasmata do not contribute to gene shuffling. Relevant species and references are: PLANTS: *Allium fitsulosum* (Dyer, 1964), *Allium cepa*, *A. consangineum*, *A. kachrooi*, and *A. nigrum* (Gohil and Kaul, 1980), *Crepis capillaris* (Brown and Jones, 1976), *Festuca mairei* (Malik and Tripathi, 1970), *Fritillaria acmopetala* (Frankel, 1940), *Fritillaria longiflorum*, *F. meleagris*, and *F. martagon* (Fogwill, 1958), *Listera ovata* (Vosa and Barlow, 1972), *Lolium perenne* (Cameron and Rees, 1967; Karp and Jones, 1982), *Puschkinia libanotica* (Barlow and Vosa, 1970), *Secale cereale* (Jones and Rees, 1967; Zecevic and Paunovic, 1969), *Trillium kamtschaticum* (Dyer, 1964), *Zea mays* (Ayonoadu and Rees, 1968). ANIMALS: *Bryodema tuberculata* (Henderson, 1969), *Ceratophrys cranwelli* and *C. ornata* (Rahn and Martinez, 1983), *Culmacris archaica* (White, 1979), *Dendrocoelum lacteum* (Pastor and Callan, 1952), *Euthystira brachyptera* (Fletcher and Hewitt, 1980), *Mesostoma ehrenbergii ehrenbergii* (Oakley and Jones, 1982; Oakley, 1982), *Mus musculus* (Polani, 1972), *Myrmeleotettix maculatus* (Hewitt, 1976), *Odontophrynus americanus* (Rahn and Martinez, 1983), *Parapleurus alliaceus* (White, 1954; Fletcher and Hewitt, 1980), *Smithopsis crassicaudata* (Bennett et al., 1986), *Spectriforma gracillicollis* (White, 1977), *Stethophyma grossum* (Shaw, 1971; Perry and Jones, 1974), *Tetrix ceperoi* (Henderson, 1961), *Triturus cristatus* (Watson and Callan, 1963), *Triturus helveticus* (Callan and Perry, 1977). These data were cited from the tables 2.2, 2.4, 2.10, and 7.1 in the text by John (1990).

### *C. Reconsideration of the chiasma frequency per cell (FX)*

Chiasma frequency per cell (in our terminology FX) has been conventionally estimated in organisms with relatively low chromosome numbers ($n \leqq 12$). Because past estimations include both interstitial (Xi) and terminal chiasma (Xt), the conventional term FX corresponds to FXit in this paper. As far as the data listed by John (1990) are concerned, the FXit values correlate linearly with the number of bivalents (= haploid chromosome number, n) (Fig. 15a). Note that the slope is very steep (FXit≈2n).

We have emphasized in previous sections that Xi can contribute to gene shuffling, whereas Xt is a mechanism serving to bind the termini of bivalents. If this is true, FXit values would tend to be overestimated. In order to minimize such overestimations we propose that FXi should be used in analysis rather than FXit.

We have examined the difference between FXi and FXit at diakinesis by using Chinese hamsters (n=11), mice (n=20), and dogs (n=39). Diakinesis is the best cell stage for estimation of chiasma frequency; since pseudochiasmata formation as a result of the twisting of bivalents at diplotene has ceased and pseudoterminalization is less prominent than in Metaphase I. The results are summarized in Fig. 15b, where FXit values are always higher than FXi values. The degree of difference is less extreme in Chinese hamsters, with their relatively low chromosome number (FXit=FXi+2; Fig. 15b-1), than in the domestic dog, which has a relatively high chromosome number (FXit=FXi+15; Fig. 15b-4).

With regard to this, Hulten (1974) estimated FXit=50.61±3.87 for the human male (n=23; Fig. 15b-3). This value is about three times higher than that of mice with a comparable chromosome number (FXi=17.1±2.3; Imai and Moriwaki, 1982; also see Fig. 15b-2 open circle). We conclude that this overestimation by Hulten results from the prominence of terminal chiasmata (Xt) in metacentric bivalents (see Fig. 7 of Hulten, 1974). In a metacentric bivalent with one Xi and two Xt (1Xi.2Xt in our terminology), chiasma frequency per bivalent is FXit/b=3, but FXi/b=1. Since the human karyotype is rich in metacentrics, one can expect approximately FXi≈FXit/3=50.6÷3=16.9, which is almost comparable to FXi=17.1 in mice! The same arguments are applicable to the other examples shown in Fig. 15a. It must be concluded that critical reexamination of conventional chiasma frequency is required.

### *D. Crossing-over as the prime-mover of chromosome evolution*

Imai et al. (1986) proposed the minimum interaction theory for eukaryotic chromosome evolution. The essence of the theory is that, overall chromosome evolution proceeds toward increase in chromosome numbers by centric fission, with the biological function of minimizing deleterious chromosomal mutations such as reciprocal translocations. Evidence supporting this theory has been accumulated by Hirai et al. (1994), Imai (1991), and Imai et al. (1988, 1994).

Crossing-over is recognized in the minimum interaction theory as one of the major mechanisms inducing spontaneous chromosomal mutations. If crossing-over is principally a random event, it is possible to estimate the occurrence rates of chromosomal mutations using the Monte Carlo simulation method, and then theoretically to analyze any overall tendencies in chromosome evolution. This has already been effected by Imai et al. (1986).

Despite our expectations, conventional chiasma analyses were too descriptive and enumerative. Their most evident defect is that information regarding chiasma distribution on bivalents and chiasma frequency per cell were biased because of assumptions concerning chiasma terminalization, or because of the computation of terminal chiasma (Xt), as discussed above.

As far as the chiasma frequencies (FXit) presented in Fig. 15a are concerned, there is a strong linear correlation between FXit and haploid chromosome number (n), FXit$\approx$2n. Following the minimum interaction theory this means that chromosomally derived species (those with high chromosome numbers) have high FXit values. This conclusion is both attractive and reasonable, if the rates of occurrence of spontaneous chromosomal mutations are a function of (or proportional to) FXit. However, as indicated above, FXit values are prone to overestimation, especially in species with $n>10$ (Fig. 15b, solid circles). Thus, we propose FXi instead of FXit be used in relevant analyses.

In Fig. 15b, the FXi value tends also to increase slightly as chromosome numbers increase (open circles), but there is an alternative possibility, namely that the value is roughly constant in mammals (FXi$=20\pm5$). Although further investigations are required to support a more satisfactory conclusion, we emphasize that chiasma analysis can provide essential information for understanding the mechanisms of eukaryotic chromosome evolution.

We thank Mr. H. Uda for his invaluable support and encouragement to our study, and Drs Y. Matsuda and M.-T. Yamamoto for providing valuable information on X-Y association in mammals and on *Drosophila* genetics. We also thank Drs M. M. Green, R. W. Taylor, and K. Oishi for their critical reading of the manuscript and offering valuable suggestions.

## REFERENCES

Ashley, T., Jaarola, M. and Fredga, K. (1989). The behavior during pachynema of a normal and an inverted Y chromosome in *Microtus agrestis*. *Hereditas* **111**, 281–294.

Belling, J. (1931). Chiasma in flowering plants. *Univ. California Publ. Botany* **16**, 311–338.

Brown, W. R. A. (1988). A physical map of the human autosomal region. *EMBO J.* **7**, 2377–2385.

Charles, D. R. (1938). The spatial distribution of cross-overs in X-chromosome tetrads of *Drosophila melanogaster*. *J. Genet.* **36**, 103–126.

Darlington, C. D. (1932). *Recent Advances in Cytology*. Churchill, London.

Darlington, C. D. (1933). The origin and behaviour of chiasmata. VIII. *Secale cereale* (n, 8). *Cytologia* **4**, 444–452.

Evans, C. W. and Dickinson, H. G. (1984). *Controlling Events in Meiosis.* The Company of Biologists Limited, Cambridge.

Evans, E. P., Burtenshaw, M. D. and Cattanach, B. M. (1982). Meiotic crossing-over between the X and Y chromosomes of male mice carrying the sex reversing (*Sxr*) factor. *Nature* **300**, 443–445.

Foss, E., Lande, R., Stahl, F. W. and Steinberg, C. M. (1993). Chiasma interference as a function of genetic distance. *Genetics* **133**, 681–691.

Fox, D. P. (1973). The control of chiasma distribution in the Locust, *Schistocerca gregaria* (Forskal). *Chromosoma* **43**, 289–328.

Glamann, J. (1986). Crossing over in the male mouse as analysed by recombination nodules and bars. *Carlsberg Res. Commun.* **51**, 143–162.

Goetz, P., Chandley, A. C. and Speed, R. M. (1984). Morphological and temporal sequence of meiotic prophase development at puberty in the male mouse. *J. Cell Sci.* **65**, 249–263.

Hirai, H., Yamamoto, M. -T., Ogura, K., Satta, Y., Yamada, M., Taylor, R. W. and Imai, H. T. (1994). Multiplication of 28S rDNA and NOR activity in chromosome evolution among ants of the *Myrmecia pilosula* species complex. *Chromosoma* **103**, 171–178.

Hobolth, P. (1981). Chromosome pairing in allohexaploid wheat var. Chinese Spring. Transformation of multivalents into bivalents, a mechanism for exclusive bivalent formation. *Carlsberg Res. Commun.* **46**, 129–173.

Holm, P. B. and Rasmussen, S. W. (1980). Chromosome pairing, recombination nodules and chiasma formation in diploid *Bombyx* males. *Carlsberg Res. Commun.* **45**, 483–548.

Howell, W. M. and Black, D. A (1980). Controlled silver-staining of nucleus organizer region with a protective colloidal developer: a 1-step method. *Experientia* **36**, 1014–1015.

Hulten, M. (1974). Chiasma distribution at diakinesis in the normal human male. *Hereditas* **76**, 55–78.

Imai, H. T. (1991). Mutability of constitutive heterochromatin (C-bands) during eukaryotic chromosomal evolution and their cytological meaning. *Jpn. J. Genet.* **66**, 635–661.

Imai, H. T. and Moriwaki, K. (1982). A re-examination of chiasma terminalization and chiasma frequency in male mice. *Chromosoma* **85**, 439–452.

Imai, H. T., Taylor, R. W. and Crozier, R. H. (1994). Experimental bases for the minimum interaction theory. I. Chromosome evolution in ants of the *Myrmecia pilosula* species complex (Hymenoptera: Formicidae: Myrmiciinae). *Jpn. J. Genet.* **69**, 137–182.

Imai, H. T., Matsuda, Y., Shiroishi, T. and Moriwaki, K. (1981). High frequency of X-Y chromosome dissociation in primary spermatocytes of $F_1$ hybrids between Japanese wild mice (*Mus musculus molossinus*) and inbred laboratory mice. *Cytogenet. Cell Genet.* **29**, 166–175.

Imai, H. T., Maruyama, T., Gojyobori, T., Inoue, Y. and Crozier, R. H. (1986). Theoretical bases for karyotype evolution. I. The minimum-interaction hypothesis. *Am. Nat.* **128**, 900–920.

Imai, H. T., Takahata, N., Maruyama, T., Daniel, A., Honda, T., Matuda, Y. and Moriwaki, K. (1988). Theoretical bases for karyotype evolution. II. The fusion burst in man and mouse. *Jpn. J. Genet.* **63**, 313–342.

Janssens, F. A. (1924). La chiasmatype dans les insectes. *La Cellule* **34**, 135–359.

John, B. (1990). *Meiosis.* Cambridge Univ. Press, Cambridge.

John, B. and King, M. (1982). Meiotic effects of supernumerary heterochromatin in *Heteropternis obscurella. Chromosoma* **85**, 39–65.

John, B. and King, M. (1985). Pseudoterminalisation, terminalisation and the origin of terminal associations. *Chromosoma* **93**, 89–99.

John, B. and Miklos, G. L. G. (1979). Functional aspects of satellite DNA and heterochromatin. *Int. Rev. Cytol.* **58**, 1–114.

Jones, G. H. (1974). Correlated components of chiasma variation and the control of chiasma distribution in rye. *Heredity* **32**, 375–387.

Jones, G. H. (1978). Giemsa C-banding of rye meiotic chromosomes and the nature of "terminal" chiasmata. *Chromosoma* **66**, 45–57.

Jones, G. H. (1984). The control of chiasma distribution. In: *Controlling Events in Meiosis* (eds.: C.W. Evans and H.G. Dickinson), *Symp. Soc. Exp. Biol.* **38**, 293–320.

Jones, G. H. and Tease, C. (1984). Analysis of exchanges in differentially stained meiotic chromosomes of *Locusta migratoria* after BrdU-substitution and FPG staining. IV. The nature of "terminal" associations. *Chromosoma* **89**, 33–36.

Joseph, A. M. and Chandley, A. C. (1984). The morphological sequence of XY pairing in the Norway rat *Rattus norvegicus*. *Chromosoma* **89**, 381–386.

Kanda, N. and Kato, H. (1980). Analysis of crossing-over in mouse meiotic cells by BrdU labelling technique. *Chromosoma* **78**,113–122.

Keitges, E., Rivest, M., Siniscalco, M. and Gartler, S. M. (1985). X-linkage of steroid sulphatase in the mouse is evidence for a functional Y-linked allele. *Nature* **315**, 226–227.

King, J. S. and Mortimer, R. K. (1990). A polymerization model of chiasma interference and corresponding computer simulation. *Genetics* **126**, 1127–1138.

Kipling, D., Wilson, H. E., Mitchell, A. R., Taylor, B. A. and Cooke, H. J. (1994). Mouse centromere mapping using oligonucleotide probes that detect variants of the minor satellite. *Chromosoma* **103**, 46–55.

Lande, R. and Stahl, F. W. (1993). Chiasma interference and the distribution of exchanges in *Drosophila melanogaster*. *Cold Spring Harbor Symp. Quant. Biol.* **58**, 543–552.

Lindsley, D. L. and Sandler, L. (1977). The genetic analysis of meiosis in female *Drosophila melanogaster*. *Phil. Trans. R. Soc. London* **B277**, 295–312.

Masumoto, H., Sugimoto, K. and Okazaki, T. (1989a). Alphoid satellite DNA is tightly associated with centromere antigens in human chromosomes throughout the cell cycle. *Exp. Cell Res.* **181**, 181–196.

Masumoto, H., Masukata, H., Muro, Y., Nozaki, N. and Okazaki, T. (1989b). A human centromere antigen (CENP-B) interacts with a short specific sequence in alphoid DNA, a human centromeric satellite. *J. Cell Biol.* **109**, 1963–1973.

Mather, K. (1936). The determination of position in crossing-over. I. *Drosophila melanogaster*. *J. Genet.* **33**, 207–235.

Mather, K. (1937). The determination of position in crossing-over. II. The chromosome length-chiasma frequency relation. *Cytologia (Tokyo)* **Fujii Jubilee Volume**, 514–526.

Maudlin, I. and Evans, E. P. (1980). Chiasma distribution in mouse oocytes during diakinesis. *Chromosoma* **80**, 49–56.

Meyne, J., Baker, R. J., Hobart, H. H., Hsu, T. C., Ryder, O. A., Ward, O. G., Wiley, J. E., Wurster-Hill, D. H., Yates, T. L. and Moyzis, R. K. (1990). Distribution of non-telomeric sites of the $(TTAGGG)_n$ telomeric sequence in vertebrate chromosomes. *Chromosoma* **99**, 3–10.

Miklos, G. L. G. and Nankivell, R. N. (1976). Telomeric satellite DNA functions in regulating recombination. *Chromosoma* **56**, 143–167.

Moens, P. B. (ed.) (1987). *Meiosis*. Academic Press, London.

Moens, P. B. and Pearlman, R. E. (1990). Telomere and centromere DNA are associated with the cores of meiotic prophase chromosomes. *Chromosoma* **100**, 8–14.

Morgan, T. H. (1910). Sex-limited inheritance in *Drosophila*. *Science* **32**, 120–122.

Morton, N. E., Rao, D. C. and Yee, S. (1976). An inferred chiasma map of *Drosophila melanogaster*. *Heredity* **37**, 405–411.

Moyzis, R. K., Buckingham, J. M., Cram, L. S., Dani, M., Deaven, L. L., Jones, M. D., Meyne, J., Ratliff, R. L. and Wu, J. -R. (1988). A highly conserved repetitive DNA sequence, $(TTAGGG)_n$, present at the telomere of human chromosomes. *Proc. Natl. Acad. Sci. USA* **85**, 6622–6626.

Petit, C., Levillies, J. and Weissenbach, J. (1988). Physical mapping of the human pseudoautosomal region: comparison with genetic linkage map. *EMBO J.* **7**, 2369–2376.

Rasmussen, S. W. and Holm, P. B. (1984). The synaptonemal complex, recombination nodules and chiasmata in human spermatocytes. In: *Controlling Events in Meiosis* (eds.: C. W. Evans and H. G. Dickinson), *Symp. Soc. Exp. Biol.* **38**, 271–292.

Rouyer, F., Simmler, M. C., Johnsson, C., Vergnaud, G., Cooke, H. J. and Weissenbach, J. (1986). A gradient of sex linkage in the pseudoautosomal region of the human sex chromosomes. *Nature* **319**, 291–295.

Sax, K. (1930). Chromosome structure and the mechanism of crossing over. *J. Arnord Arbor. Harv. Univ.* **11**, 193–220.

Sharp, P. (1982). Sex chromosome pairing during male meiosis in marsupials. *Chromosoma* **86**, 27–47.

Solari, A. J. (1970). The spatial relationship of the X and Y chromosomes during meiotic prophase in mouse spermatocytes. *Chromosoma* **29**, 217–236.

Solari, A. J. (1988). Synaptic behaviour and recombination nodules in the human XY pair. *Genetica* **77**, 149–158.

Solari, A. J. (1994). *Sex Chromosomes and Sex Determination in Vertebrates.* CRC Press, Boca Raton, Florida.

Solari, A. J. and Ashley, T. (1977). Ultrastructure and behavior of the achiasmatic, telosynaptic XY pair of the sand rat (*Psammomys obesus*). *Chromosoma* **62**, 319–336.

Southern, D. I. (1967). Chiasma distribution in Truxaline grasshoppers. *Chromosoma* **22**, 164–191.

Stack, S. M. and Anderson, L. K. (1986). Two-dimensional spreads of synaptonemal complexes from solanaceous plants. III. Recombination nodules and crossing over in *Lycopersicon esculentum* (tomato). *Chromosoma* **94**, 253–258.

Sturtevant, A. H. (1913). The linear arrangement of six sex-linked factors in *Drosophila*, as shown by their mode of association. *J. Exp. Zool.* **14**, 43–59.

Suja, J. A. and Rufas, J. S. (1994). The telochore: a telomeric differentiation of the chromosome axis. *Chr. Res.* **2**, 361–368.

Sumner, A. T. (1990). *Chromosome Banding.* Unwin Hyman Ltd., London.

Tease, C. and Jones, G. H. (1978). Analysis of exchanges in differentially stained meiotic chromosomes of *Locusta migratoria* after BrdU-substitution and FPG staining. I. Crossover exchanges in monochiasmate bivalents. *Chromosoma* **69**, 163–178.

Tres, L. L. (1977). Extensive pairing of the XY bivalent in mouse spermatocytes as visualized by whole-mount electron microscopy. *J. Cell Sci.* **25**, 1–15.

Ved Brat, S. and Rai, K. S. (1973). An analysis of chiasma frequencies in *Aedes aegypti*. *Nucleus* **16**, 184–193.

Wada, M. Y. and Imai, H. T. (1991). On the Robertsonian polymorphism found in the Japanese raccoon dog (*Nyctereutes procyonoides viverrinus*). *Jpn. J. Genet.* **66**, 1–11.

Wettstein, D. von (1984). The synaptonemal complex and genetic segregation. In: *Controlling Events in Meiosis* (eds.: C. W. Evans and H. G. Dickinson), *Symp. Soc. Exp. Biol.* **38**, 195–231.

Wolf, K. W., Baumgart, K. and Winking, H. (1988). Meiotic association and segregation of the achiasmatic giant sex chromosomes in the field vole (*Microtus agrestis*). *Chromosoma* **97**, 124–133.

Yamamoto, M. and Miklos, G. L. G. (1978). Genetic studies on heterochromatin in *Drosophila melanogaster* and their implications for the functions of satellite DNA. *Chromosoma* **66**, 71–98.

Zickler, D. (1977). Development of the synaptonemal complex and the "recombination nodules" during meiotic prophase in the seven bivalents of the fungus *Sordaria macrospora* Auersw. *Chromosoma* **61**, 289–316.